ANNUAL REVIEWS

Annual Review of Biophysics

Membrane Electroporation and Electropermeabilization: Mechanisms and Models

Tadej Kotnik,[1] Lea Rems,[2] Mounir Tarek,[3] and Damijan Miklavčič[1]

[1]Faculty of Electrical Engineering, University of Ljubljana, SI-1000 Ljubljana, Slovenia; email: tadej.kotnik@fe.uni-lj.si, damijan.miklavcic@fe.uni-lj.si

[2]Science for Life Laboratory, Department of Applied Physics, KTH Royal Institute of Technology, 17165 Solna, Sweden; email: lea.rems@scilifelab.se

[3]Université de Lorraine, CNRS, LPCT, F-54000 Nancy, France; email: mounir.tarek@univ-lorraine.fr

Annu. Rev. Biophys. 2019. 48:63–91

First published as a Review in Advance on February 20, 2019

The *Annual Review of Biophysics* is online at biophys.annualreviews.org

https://doi.org/10.1146/annurev-biophys-052118-115451

Keywords

pulsed electric field treatment, cell membrane, aqueous pores in lipid bilayers, transmembrane molecular transport, theoretical model, molecular dynamics

Abstract

Exposure of biological cells to high-voltage, short-duration electric pulses causes a transient increase in their plasma membrane permeability, allowing transmembrane transport of otherwise impermeant molecules. In recent years, large steps were made in the understanding of underlying events. Formation of aqueous pores in the lipid bilayer is now a widely recognized mechanism, but evidence is growing that changes to individual membrane lipids and proteins also contribute, substantiating the need for terminological distinction between electroporation and electropermeabilization. We first revisit experimental evidence for electrically induced membrane permeability, its correlation with transmembrane voltage, and continuum models of electropermeabilization that disregard the molecular-level structure and events. We then present insights from molecular-level modeling, particularly atomistic simulations that enhance understanding of pore formation, and evidence of chemical modifications of membrane lipids and functional modulation of membrane proteins affecting membrane permeability. Finally, we discuss the remaining challenges to our full understanding of electroporation and electropermeabilization.

Contents

Electro-permeabilization: electrically induced increase in the membrane permeability for molecules devoid of physiological mechanisms of transmembrane transport

Electroporation: electrically induced formation of aqueous pores in the lipid bilayer under the influence of the induced transmembrane voltage

1. INTRODUCTION

Exposure of biological cells and tissues to short electric pulses, with sufficient amplitude to increase the permeability of the membrane, is an increasingly relevant technique in biomedicine (215), biotechnology (94), food science and technology (65), and environmental science (116). In different fields of application, this technique is referred to as electropermeabilization, electroporation, electropulsation, or PEF (pulsed electric field) treatment, with nuanced differences in the prevailing definition of each, as outlined in the margin.

Similarly, the underlying phenomenon is itself termed either electroporation or electropermeabilization, often used as synonyms, while more rigorously, the former term is narrower and refers only to the contribution to the increased permeability of the membrane owing to the formation of aqueous pores in its lipid bilayer, while the latter is more general and ascribes this increase to a broader range of (bio)physical and (bio)chemical mechanisms. Although formation of transient hydrophilic pores in the lipid bilayer (i.e., electroporation in the narrow sense) is now a widely recognized mechanism of membrane permeabilization, governed by statistical thermodynamics and corroborated by molecular dynamics (MD) simulations, there is increasing evidence that exposure to electric pulses also causes chemical changes to the lipids and modulation of membrane proteins' function that contribute to the membrane's increased permeability.

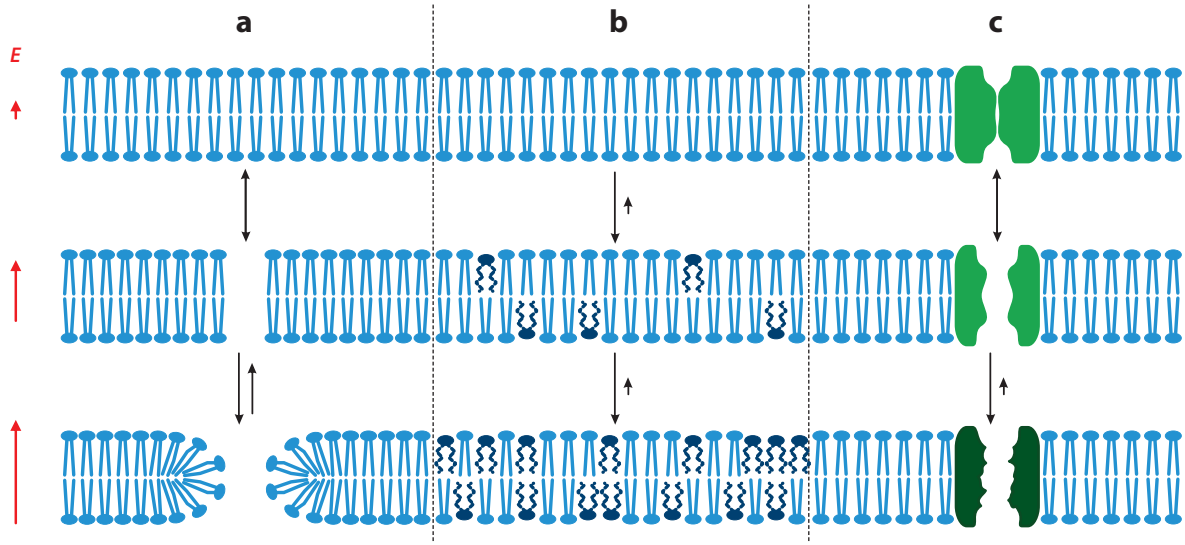

Figure 1

Conceptual scheme of molecular-level mechanisms of electropermeabilization, starting from an intact membrane (*top*). (*a*) Electroporation: electrically induced formation of aqueous pores in the lipid bilayer, shown here in two stages, with water molecules first penetrating the bilayer and thus forming an unstable hydrophobic pore (*middle*), and with adjacent lipids then reorienting with their polar headgroups toward these water molecules and thus forming a metastable hydrophilic pore (*bottom*). (*b*) Electrically induced chemical changes to membrane lipids, including peroxidation, which deforms their tails and increases the bilayer's permeability to water, ions, and small molecules. (*c*) Electrically induced modulation of membrane proteins' function, shown here for a voltage-gated channel. Arrow lengths for the electric field (*E*, *red*) correspond to its strength (i.e., amplitude of the electric pulse or pulses), while those for transitions between states of membrane permeability reflect the transition rate (shorter arrow = slower rate; not drawn to scale between the three mechanisms).

The aim of this review is to present and discuss the current theoretical understanding and experimental knowledge of the mechanisms contributing to the increase in membrane permeability of cells and tissues exposed to electric pulses, with the underlying molecular-level events outlined schematically in **Figure 1**.

Electropulsation [also PEF (pulsed electric field) treatment]: exposure of cells to electric pulses, leading to their membranes' structural alteration and increased conductivity and/or permeability

Induced transmembrane voltage (induced TMV): increase in transmembrane voltage resulting from exposure to electric pulses and associated with an increase in transmembrane electric field

2. ELECTROPERMEABILIZATION AT THE CELL LEVEL

Nearly all cells maintain an electric potential difference between the inner and outer side of their plasma membrane, generated and regulated by a system of ion pumps and channels in the membrane, and termed the resting transmembrane voltage (TMV). In eukaryotic cells, the resting TMV typically ranges from –40 to –70 mV, in the sense that the inner potential is lower than the outer one. As this is the natural state of biological membranes, both their lipid and protein components are evolutionarily well adapted and function under voltages in this range.

2.1. Correlation Between Transmembrane Voltage and Electropermeabilization-Mediated Transport

An exposure of a cell to an external electric field results in an additional component of TMV, termed the induced TMV, sustained for the duration of the exposure and proportional to the strength of the external electric field (46, 98, 153). Thus, exposures to sufficiently strong fields can induce TMVs far exceeding their resting range and causing both structural changes to the membrane and changes to its constituent molecules that do not occur under physiological conditions.

Among the clearest and most prominent such effects is membrane electropermeabilization—a rapid and substantial increase in membrane permeability, revealed by transmembrane transport of molecules for which an intact membrane is practically impermeable (89, 99, 136, 152, 215).

A number of studies, based on both experimental and theoretical considerations, implied that the molecular flow across the electropermeabilized membrane is largely limited to the regions of the membrane exposed to sufficiently high TMV (56, 57, 73, 74, 89, 193, 199). This was conclusively shown experimentally, for a single cell as well as clusters of cells, by monitoring both the TMV and the transmembrane transport on the same cells upon their exposure to electric pulses (99), as shown in **Figure 2**.

2.2. Kinetics of Electropermeabilization-Mediated Transport and Factors of Influence

The main consequence of membrane electropermeabilization is the inflow of membrane-impermeant molecules into the cell and the outflow of biomolecules from the cell. The kinetics of transmembrane transport mediated by electropermeabilization have thus been studied extensively, revealing that membrane electrical conductivity and permeability increase detectably within less than a microsecond after the onset of the electric pulse, provided that the TMV exceeds a certain "critical" value, with quotation marks used as it is not a universal constant but a variable dependent on a number of factors. Still, to start with the general observations, the experimentally determined kinetics of transmembrane transport can roughly be divided into five stages, as summarized in **Table 1**: the initiation of the permeable state, its expansion, stabilization with partial recovery, the resealing of the membrane, and finally gradual cessation of what are referred to as residual memory effects reflected in cells' altered physiological processes and reactions to various stressors.

From a theoretical perspective, electropermeabilization of the membrane—be it the consequence of structural rearrangement of its lipids, or chemical modifications of its lipids or functional modulation of its proteins, or a combination thereof—is not strictly a threshold event, in the sense that these processes would occur only in an electric field exceeding a certain value; at most, the rates of these processes increase nonlinearly with the increase in the field amplitude to which the cells are exposed. Still, empirically, for each type of cells, type of molecules transported, exposure duration, and particular set of conditions such as temperature, there is a critical value of the field that must be exceeded for electropermeabilization-mediated transport to become detectable, and there is another, higher critical value of the field that must not be exceeded if membrane stabilization, recovery, and resealing are still to occur. As a consequence, experimentalists often treat electropermeabilization as a quasi-threshold phenomenon, yet the two critical values of the field between which permeabilization is detectable as well as reversible depend on so many factors that only their orders of magnitude can be stated generally. Thus, for eukaryotic cells, detection occurs for electric fields resulting in TMV in hundreds of millivolts and irreversible damage for electric fields $\sim$3–5$\times$ higher than the minimum for detection (56, 99, 190, 199).

As mentioned above, the critical electric field and the corresponding TMV for detectable electropermeabilization depend on the cell type (24), transported molecule (151, 165), and exposure duration (73, 151, 165) and are also influenced by cell size and local membrane curvature (71, 82, 199), temperature (86, 146), and osmotic pressure (66), and artifactually by the sensitivity of the detection technique (95, 137, 209).

Direct microscopic observations reveal that electropermeabilization-mediated transport is highly dependent on the size and charge of the molecules. Small molecules can thus enter the

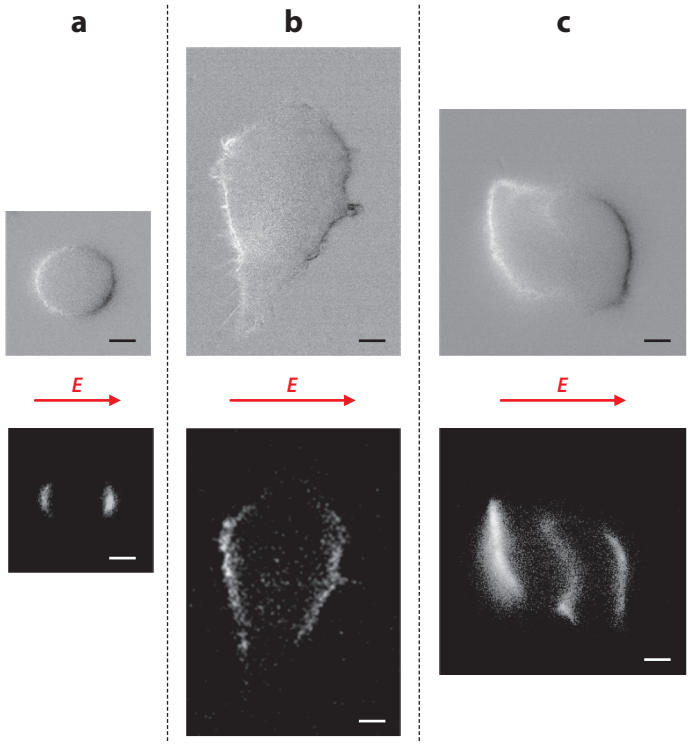

Figure 2

The transmembrane voltage (TMV) (*top*) and electropermeabilization (*bottom*) of Chinese hamster ovary cells in a physiological medium. The TMV was monitored by di-8-ANEPPS, a potentiometric dye, and electropermeabilization was monitored by propidium iodide (PI), a dye highly impermeant to an intact membrane and fluorescing only inside the cell. (*a*) A nearly spherical cell suspended in the medium, electroporated by a single 1.5-ms, 650-V/cm pulse. (*b*) An irregularly shaped cell attached to a flat surface, electroporated by a single 200-μs, 1,000-V/cm pulse. (*c*) A pair of cells in close contact and attached to a flat surface, electroporated by a single 200-μs, 1,000-V/cm pulse. In the TMV images (i.e., di-8-ANEPPS fluorescence), the brightest and darkest regions of the membrane correspond to the highest positive and highest negative TMV, respectively. In the electropermeabilization images (i.e., PI fluorescence), the brightest and darkest regions correspond to the highest and lowest concentrations, respectively, of internalized PI. In panel *c*, the TMV along the contact between the two cells is obscured, as there, their membranes are oppositely charged (positive TMV in the cell at the left, negative TMV in the cell at the right), so the two fluorescence signals partly cancel each other, but the PI fluorescence in these regions shows that permeabilization occurs also there. All panels are drawn to scale, with the bar corresponding to 5 μm. Additional abbreviation: *E*, electric field. Figure adapted from Reference 99 with permission.

cell both during and after the pulse, and through the membrane regions with sufficiently high negative or sufficiently high positive TMV (see **Figure 2**). For charged species, the entry during the pulse is mostly electrophoretic and proceeds, for the given net charge, from the side with the opposite polarity of TMV, while after the pulse, it is mostly diffusive and proceeds from both sides (57, 58, 152), but recent experiments also suggest a nonnegligible contribution of post-pulse TMV recovery in the transport of small charged species (181). Larger and/or multiply charged molecules enter only during the pulse and only from the side with the opposite polarity of TMV (e.g., multiply negatively-charged oligonucleotides enter from the side with positive TMV) (136). For still larger molecules, such as plasmid DNA, electropermeabilization initializes only

Table 1 Stages of electropermeabilization

Stage	Timescale	References
Initiation: Membrane electrical conductivity and permeability start increasing detectably when transmembrane voltage (TMV) exceeds a "critical" value.	Nanoseconds (conductivity) Microseconds (permeability)	52, 73, 74, 152
Expansion: As long as TMV remains above the "critical" value, conductivity and permeability persist and/or intensify.	Until the end of the pulse (up to milliseconds)	73, 74, 141, 152
Partial recovery: After TMV drops below the "critical" value, membrane conductivity and permeability decrease rapidly but not fully, stabilizing at a detectably increased level and still allowing transmembrane diffusion of ions and molecules.	Microseconds (conductivity) Milliseconds (permeability)	73, 150, 152
Resealing: The membrane gradually recovers its physiological level of impermeability (unless damage was irreversible and cell loses viability).	Seconds to minutes (~20–37°C) Hours (~4°C)	115, 134, 152, 165, 175
Memory: Even after full membrane resealing, the cell can exhibit alterations in its physiological processes and reactions to stressors before finally returning fully to its normal state.	Hours	54, 162

the transport, with longer (approximately milliseconds) pulses generally required for sufficient electrophoretic drag on DNA to enable DNA–membrane interaction (124, 165, 211). The subsequent DNA uptake is a much slower process, involving endocytotic uptake into the cytosol and intracellular trafficking to the nucleus (67, 166). A much more detailed treatise on the molecule-dependent specifics of electropermeabilization-mediated transport is provided in section II.C of Reference 157.

2.3. Submicrosecond Pulses and Intracellular Effects

Both theoretical analysis and potentiometric measurements show that at physiological salt concentration, the process of TMV inducement by rectangular pulses, mainly due to the charging of the membrane that is acting as a capacitor, is completed within several microseconds (73, 74, 98). For pulses exceeding this duration, the TMV on the cell plasma membrane—if insufficient for electropermeabilization—stabilizes at a plateau level that persists until the end of the pulse, and subsequently its induced component decays exponentially, again within microseconds.

In contrast, for submicrosecond electric pulses, the TMV does not reach this plateau, as the end of the pulse and the resulting exponential decay of the induced TMV precede it. As a result, with further shortening of the pulses from the submicrosecond to the nanosecond range, the amplitude of the TMV induced on the plasma membrane is increasingly attenuated (96, 98) and gradually becomes comparable to the TMV induced on organelle membranes in the cell interior (97). This could explain why with very short (tens or hundreds of nanoseconds) yet very strong pulses (millions of volts per meter, which is ten- to 100-fold higher than the amplitudes sufficient for electropermeabilization with pulse durations in the microsecond to millisecond range), some experiments imply pronounced permeabilizing effects also on the organelle membranes (7, 27, 172, 194). In mitochondria, their particularly high resting TMV to which the induced TMV on the mitochondrial membrane superimposes could also contribute to their selective electropermeabilization and to the observation that these organelles appear to be particularly affected by submicrosecond pulses (9).

2.4. Continuum Models

The earliest proposed models of electropermeabilization treated the membrane as a thin layer of dielectric liquid, which the electric field charges and thus exerts a pressure on, with membrane breakdown occurring at the pressure level that can no longer be equilibrated by the opposing pressure owing to the layer's surface tension (122), elasticity (35), or both of them combined with viscosity (44). In each of these models, the breakdown is a strictly threshold event, occurring at an exact level of membrane charging—and thus of TMV—where the equations describing the membrane at the pressure equilibrium cease to have a finite real-number solution. This addresses the empirical finding that permeabilization is detectable only at sufficient TMV, and at least in the models combining surface tension with elasticity, the breakdown TMV is on the realistic order of magnitude, in hundreds of millivolts (207). Still, none of these models provide a sensible description of the membrane once it breaks down; the singularity in its mathematical description there corresponds to one or more of the physical membrane-characterizing parameters assuming an infinite or zero value, while electropermeabilization is clearly not a true breakdown (e.g., tearing of an overstretched wire) but is generally a limited and often reversible process.

These shortcomings were largely addressed by modeling electropermeabilization as electroporation—electrically induced formation of aqueous pores in the lipid bilayer. Similarly to the breakdown models described above, the mathematical description of TMV-dependent pore formation disregards the molecular structure of the lipid bilayer and properties of its individual lipids, yet the physical depiction (**Figure 1*a***) of pore initiation, expansion, stabilization, and closure relies decisively on them and moreover offers a plausible description of the membrane also in its permeabilized state. The foundations to this approach were laid in 1975 with the first model of spontaneous hydrophilic pore formation (114), extended in 1979 to account also for TMV (1), and matured in 1988 into the standard model of electroporation that describes the change to the free energy ΔW of the membrane caused by formation of a pore of radius r in this membrane, at a TMV of magnitude U, as (64)

$$\Delta W(r,U) = \begin{cases} \Delta W_{\mathrm{o}}(r,U) = 2\pi d r \Gamma_{\mathrm{o}} \frac{I_1(r/\lambda)}{I_0(r/\lambda)} - \frac{(\varepsilon_{\mathrm{e}}-\varepsilon_{\mathrm{m}})\pi r^2}{2d} U^2; & r < r_{\min} \\ \Delta W_{\mathrm{i}}(r,U) = 2\pi r \gamma(r) - \Gamma_{\mathrm{i}} \pi r^2 - \frac{(\varepsilon_{\mathrm{e}}-\varepsilon_{\mathrm{m}})\pi r^2}{2d} U^2; & r > r_{\min} \end{cases}, \qquad 1.$$

where ΔW_{o} and ΔW_{i} are ΔW for the hydrophobic and hydrophilic state, respectively, of the pore; I_k is the modified Bessel function of kth order; $\gamma(r)$ is a function tending to $+\infty$ as $r \to 0$ so that $2\gamma(r)\pi r$ dominates ΔW_{i} for r in the subnanometer range and approaching the standardly measured value of edge tension γ as r increases beyond that range; $r_{\min}$ is the minimum radius of a hydrophilic pore (i.e., the pore radius at which $\Delta W_{\mathrm{i}} = \Delta W_{\mathrm{o}}$); and the other parameters are as listed in **Table 2**, which also provides their typical values. Applying these values and assuming an empirically reasonable (132)

$$\gamma(r) = \gamma(1 + C/r^5), \text{with } C = 1.39 \times 10^{-46}\,\mathrm{J/m^4} \qquad 2.$$

allows one to plot the curve $\Delta W(r)$ for any fixed U; **Figure 3** shows these curves for $U = 0$ mV, 150 mV, 300 mV, and 450 mV. The first minimum at $r = 0$ addresses the tendency of pores to close; the first maximum at $r \sim 0.5$ nm addresses the limitedness of spontaneous pore formation, while the second minimum at $r \sim 0.8$ nm and the second maximum at its right (both for TMV $< \sim$450 mV) address the (meta)stability of hydrophilic pores, which exist until passing either the first (pore closure) or the second maximum (irreversible breakdown). Both maxima decrease with increasing TMV, meaning that higher TMV increases the rate of pore formation, facilitates pore expansion, and increases the probability of irreversible breakdown of a bilayer. Yet an increase of

Table 2 Typical values of the parameters in electroporation models

Parameter		Symbol	Value	Explanation and/or reference
Temperature		T	37°C = 310 K	Average physiological value for cells in mammals (126)
Membrane	Thickness	d	5×10^{-9} m	63
	Characteristic length of hydrophobic interactions	λ	$\sim 1 \times 10^{-9}$ m	78
	Hydrophobic surface tension (lipid tails/water)	Γ_o	$\sim 5 \times 10^{-2}$ J/m^2	64
	Hydrophilic surface tension (lipid heads/water)	Γ_i	$\sim 1 \times 10^{-3}$ J/m^2	207
	Edge tension	γ	$\sim 2 \times 10^{-11}$ J/m	51
	Conductivity	σ_m	$\sim 3 \times 10^{-7}$ S/m	62
	Permittivity	ε_m	4.4×10^{-11} F/m	62
Extracellular medium	Conductivity	σ_e	1.2 S/m	Blood serum at $T = 37$°C (186)
	Permittivity	ε_e	7.1×10^{-10} F/m	Physiological saline at $T = 37$°C (135)

Tilde symbol (~) indicates values known only to the order of magnitude.
Abbreviations: F, farad; S, siemens.

TMV from 150 to 450 mV reduces the first maximum only by ~5% but the second maximum by ~83%, implying that facilitation of pore formation is rather weak, while facilitation of pore transition into an irreversible breakdown is stronger. Still, irreversible breakdown can be avoided even if TMV exceeds 450 mV, provided that the applied electric pulse is short enough and the TMV subsequently returns to 0 V before any of the pores have the time to expand beyond ~20 nm.

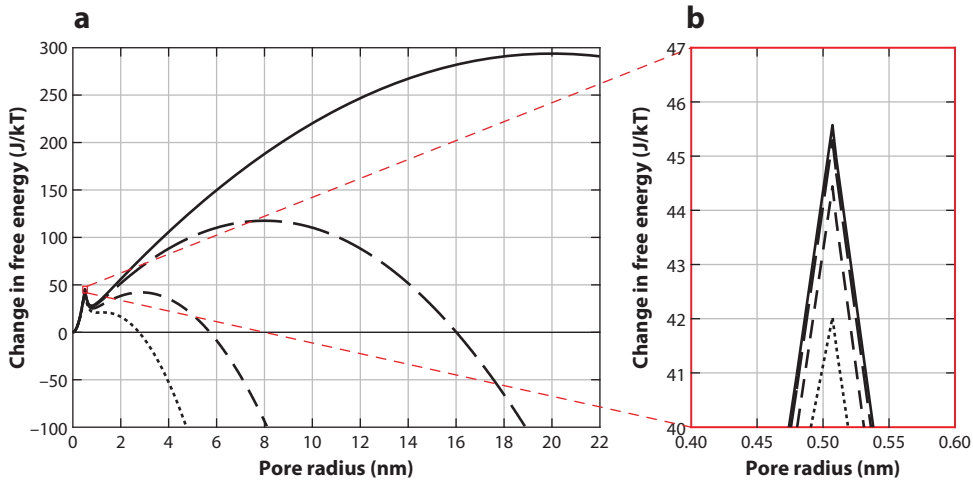

Figure 3

The change in the free energy of a pore in a lipid bilayer, according to the standard model as given by Equations 1 and 2, with parameter values as in **Table 2** at transmembrane voltage of 0 mV (*solid line*), 150 mV (*long-dashed line*), 300 mV (*short-dashed line*), and 450 mV (*dotted line*). Panel *a* shows the curves for radii up to 22 nm, and panel *b* is the zoom on the subregion outlined by the red rectangle in panel *a* and containing the first maximum of the curves.

The fate of the membrane is therefore determined by the dynamic changes of the population of pores $n(r,t)$ in the membrane, described by

$$\frac{\partial n(r,t)}{\partial t} = D_p \frac{\partial}{\partial r}\left(\frac{\partial n(r,t)}{\partial r} + \frac{n(r,t)}{kT}\frac{\partial \Delta W(r,U)}{\partial r}\right), \qquad 3.$$

where D_p is the diffusion coefficient of pores in the pore radius space, k the Boltzmann constant, and T the absolute temperature. In general, the population of pores can vary considerably for different parameters of electric pulses (6, 104, 178), and thus, numerical solution of Equation 3 needs to be obtained for each specific set of pulse parameters considered. But overall, these solutions predict that at amplitudes resulting mostly in reversible electroporation (see Section 2.3), submicrosecond pulses induce a large number (millions per cell) of small pores ($r \sim 1$ nm)—the effect sometimes termed supra-electroporation, whereas longer pulses result in a much smaller number (up to tens of thousands per cell) of pores yet with radii up to tens of nanometers (178).

Throughout the years, the quantitative description of electroporation as presented in Equations 1–3 has been subject to various modifications by different authors, as to account for the fact that a pore affects not only the capacitive but also the conductive energy of the membrane (6, 51, 104) for the difference between extracellular and cytoplasmic osmolarity (207), the effect of the membrane curvature (133), dynamic changes in the membrane surface tension caused by electroporation (176), nonlinear membrane elasticity (42), etc. Each of these proposed enhancements improved some aspects of the quantitative and/or qualitative compatibility of model predictions with experimental findings but largely at the cost of introducing a number of parameters that can—at least to date—only be evaluated by numerical fitting such as polynomial regression, and some even lack clear physical meaning. With sufficient parameter optimization, these models do yield reasonable estimates for the dynamic changes in membrane conductance during the pulse (6, 38, 51, 205) and the extent of electroporation-mediated transport (111), both resulting from the distributions of pore size and their density in the membrane, but in general, only partial quantitative agreement between model predictions and experiments is obtained. Moreover, all continuum models and analyses outlined above treat the shape of the pores as cylindrical or toroidal, which is clearly an idealization when structures and events are considered at the molecular level. Another idealization in the continuum description is its assumption that water retains its bulk properties in arbitrarily small pores; as water molecules have a van der Waals diameter of 0.28 nm, for pore sizes descending into the subnanometer range, this assumption is increasingly unrealistic. Thus, from the late 1990s, awareness was gradually emerging that further progress in understanding of electroporation will require a more realistic analysis of pore initiation, expansion, stabilization, and closure at the atomistic and molecular level, while simultaneously, computational power was gradually becoming sufficient for such analysis, to which we turn in Section 3.

Complementary molecular-level explanations of electropermeabilization have also been proposed: electrically induced phase transition of lipid molecules (184), tearing along lipid domain interfaces (36), or lipid peroxidation (11, 53, 117, 118). In a similar vein, electrically induced denaturation of membrane proteins was proposed as a companion mechanism, enhancing permeabilization in cell membranes compared to pure lipid bilayers and vesicles (200, 201). In principle, each of these models addresses the reversibility of permeabilization: phase transitions are reversible and interdomain fractures can reseal, while peroxidized lipids and denatured proteins in the membrane are gradually repaired or replaced by intact ones. Still, only electrically induced lipid peroxidation and protein denaturation have empirical support, and we revisit them in Sections 4 and 5, respectively, where we focus on chemical modification and functional modulation of membrane molecules as contributors to electropermeabilization.

3. MOLECULAR MECHANISMS OF LIPID BILAYER ELECTROPORATION

With sizes in nanometers, the pores formed in the lipid bilayer by electroporation are too small to be observable by optical microscopy, and as they are also, at most, metastable, they are too fragile to withstand the sample preparation required for electron microscopy of soft matter (vacuumization, cryofixation, or fixation by osmium tetroxide, metallic coating for scanning microscopy). Thus, an early report of volcano-shaped electropores tens of nanometers in size visualized by rapid-freezing electron microscopy (26) was later shown to be an artifact caused by sample preparation (182, 189). Visualizing the dynamics of pore formation is even more daunting, and while total internal reflection fluorescence microscopy was recently used to track ionic flux through individual pores (174), the pores were induced by pulses far longer (180 s) than any used in electroporation and recorded with temporal resolution far too slow (16 ms) to track the kinetics of pore initiation and with spatial resolution too low to discern the details of pore structure.

In contrast, MD simulations, to which we turn next, have over the last two decades reached an adequate level of both computing power and methodology proficiency to provide a corroboration of electroporation in silico. In the absence of the electric field, the rate of pore formation is generally too slow to be observable in such simulations, which typically cover a submicrosecond time span; but in sufficiently strong electric fields, the rate of pore formation increases dramatically, and pore initiation is well discernible on a nanosecond timescale.

3.1. Molecular Dynamics Modeling of Exposure to Electric Pulses

When a lipid bilayer is exposed to an electric field, the TMV induced by this exposure consists of two components: one (dielectric response) resulting from reorientation of dipoles (lipid headgroups and adjacent water molecules), on which the electric field acts as to align them, and another resulting from redistribution of charges (ions in the surrounding solutions), which the electric field drives as to accumulate them on both sides of the bilayer and thus charge it as a capacitor. The first TMV component is induced within picoseconds (188, 195, 196), while the second component is much slower, only reaching its plateau within microseconds, yet at physiological ion concentrations, it is about two orders of magnitude larger; thus, for pulses much shorter than ~1 μs the first component is dominant, while for pulses far longer, the second component prevails (97, 98).

As a consequence, MD simulations of electroporation model the buildup of TMV induced by exposing a lipid bilayer to an electric pulse depending on the pulse duration. For submicrosecond pulses, the TMV is typically generated by imposing across the bilayer an electric field E, which in practice amounts to imposing on every particle that possesses a charge q_i a force equal to the product $E \cdot q_i$ (68, 168, 188, 195, 196). For pulses lasting micro- or milliseconds, the TMV is usually modeled by imposing a net difference of charges on both sides of the bilayer, achieved in practice by relocating a required number of individual ions across the bilayer (40, 41, 70).

In both methods, the currently achievable computing power and memory capacity are far too low to model whole membranes consisting of billions of lipids (furthermore surrounded by trillions of water molecules and billions of dissolved ions). This is addressed by forming a correspondingly smaller unit simulation cell, typically rectangular and consisting of hundreds to thousands of lipids and imposing onto it a suitable set of ensemble conditions and boundary conditions, elaborated in detail in two specialized recent reviews (23, 90). The size of the simulation cell needs to be selected carefully, since too small a simulation cell can affect the size of the pore induced in the bilayer (22).

3.2. Aqueous Pores: Main Characteristics

With sufficiently high TMV, when modeled by either imposing an electric field or a charge imbalance, MD simulations qualitatively largely agree—both among themselves and with empirically determined stages of electropermeabilization-mediated transmembrane transport (see **Table 1**)—in their general description of TMV-mediated pore initiation and expansion, followed by pore closure as the TMV returns to 0 (i.e., the resting potential in simulations under symmetric salt concentrations) (108, 109, 188), as summarized in **Figure 4**. In these simulations, pore formation is initiated by small so-called water fingers protruding, on both sides of the membrane, from the headgroup/glycerol region. Molecular-scale analysis of the water-driven process of pore formation has shown that water molecules initially restrained to the hydrophilic interfacial region tend to orient their dipoles along the local electric field created by the TMV and form small clusters through intermolecular hydrogen bonds, extending increasingly into the hydrophobic core of the bilayer, and finally merging to form a hydrophobic pore (also termed water wire or water column) spanning across the bilayer (41, 75, 198). Subsequently, the lipids adjacent to the water molecules inside the pore start reorienting with their polar headgroups toward these water molecules, thus stabilizing the pore into its hydrophilic state and allowing more water, as well as other polar molecules and ions, to enter. This transition from a hydrophobic to a hydrophilic pore

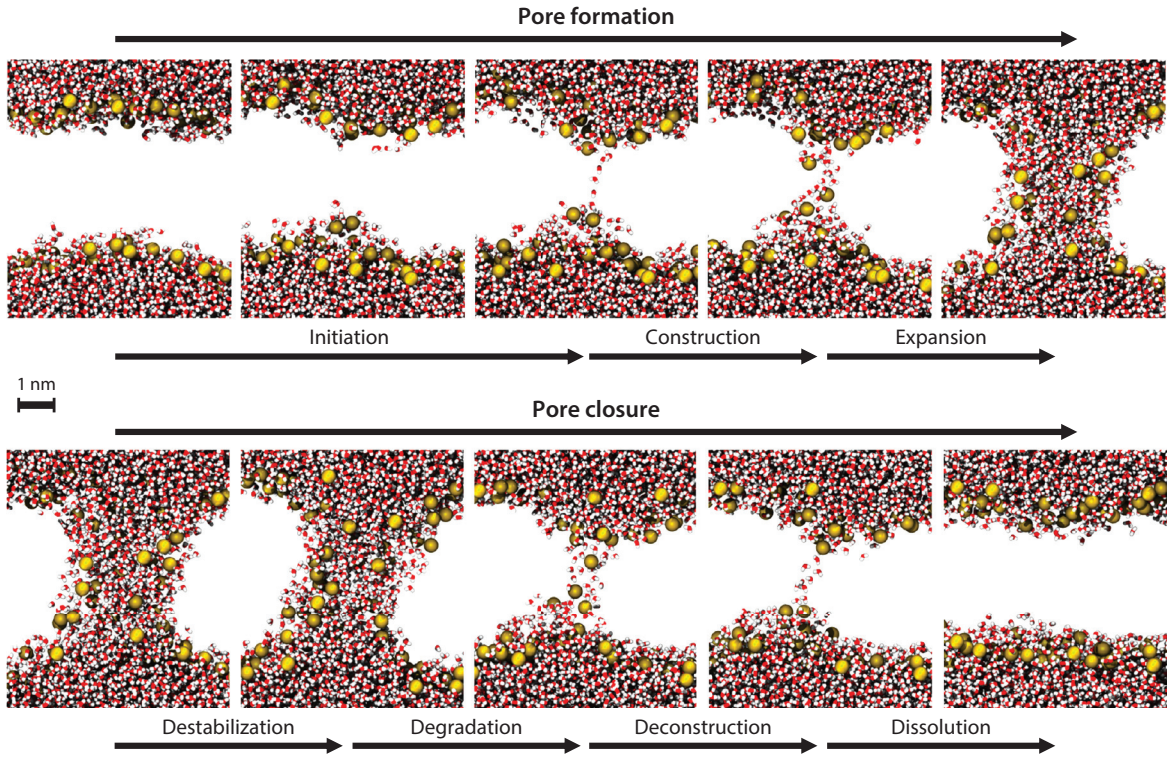

Figure 4

The life cycle of an electrically induced pore in the lipid bilayer. Stages of pore formation and closure are displayed in their order of appearance but disregarding the differences in their characteristic timescales. Formation begins with the onset of the electric field, and closure begins as the field ceases. For clarity, only water molecules and phosphorus atoms from the lipid headgroups are shown. Figure adapted from Reference 109 with permission.

structure, which was already hypothesized in the earliest electroporation models (1), can be observed in most phospholipid bilayers. However, in some bilayers (e.g., those from phosphatidylserine lipids with negatively charged headgroups or archaeal lipids with headgroups containing large sugar moieties), only hydrophobic pores were reported, which were nonetheless large enough to conduct ions (39, 146).

Once the electric field ceases, pore closure follows a reverse sequence of analogous events (**Figure 4**). Unlike pore initiation time, which decreases exponentially with increasing electric field and TMV, pore closure time is practically independent of the field by which the pore was induced (108). Pore closure is completed within tens to hundreds of nanoseconds (10, 108, 188), indicating that pores are unstable if TMV is absent or very low and only become (meta)stable for TMV of several hundred millivolts (22, 49), in agreement with measurements on model lipid bilayers (120, 174). The pore closure time in MD simulations is, however, about nine orders of magnitude shorter than typical experimentally determined membrane resealing times (see **Table 1**). This suggests either that the pores in cell membranes are more complex than lipidic pores studied in MD (208) or that, in addition to electroporation, electropermeabilization of cell membranes may involve other mechanisms, which we discuss in Sections 4 and 5.

3.3. Role of Bilayer Composition in Electroporation Thresholds

Pore formation is not strictly a threshold phenomenon (pore initiation time decreases with increasing electric field and TMV); nevertheless, we can define a threshold electric field and TMV in which electroporation is observed in a given amount of time. MD provided a molecular basis for the experimentally observed difference in electroporation thresholds in bilayers with different composition (102, 204). Since the pioneering simulations (188, 195, 196), which considered single-component zwitterionic lipid bilayers, a variety of lipid bilayer compositions have been modeled to characterize the key elements that might modulate their electroporation thresholds. The increase of the electroporation threshold upon addition of cholesterol, often linked to the increase of the stiffness of the bilayer, was studied (21, 47, 81, 92). For pulses in the submicrosecond duration range, a doubling of the electric field strength was necessary for electroporation of bilayers with 50 mol% phospholipids replaced by cholesterol (47), while for pulses with durations in the microsecond to millisecond range, the threshold was shown to level off above 30 mol% cholesterol (21). An interesting aspect emerged from modeling bilayer patches comprising liquid ordered and liquid disordered domains (156): Pore formation appeared to occur in the disordered phase without affecting the boundaries between the two phases. This behavior has been confirmed using optical recording that allows tracking of multiple isolated electropores in real time in planar droplet interface bilayers (174).

The effects of ester and ether linkages of branched (phytanoyl) tails and of bulky (glucosyl-myo and myo-inositol) lipid headgroups on the electroporation threshold were also investigated (145, 146). It was shown that the threshold for a lipid bilayer depends not only on its capacitance and dipole potential but also on the nature of lipids' hydrophobic tails. Furthermore, there is a correlation between the lateral pressure within the lipid core and the electroporation threshold, and an increase of this pressure in branched lipid membranes compared with acyl chain lipid bilayers hinders the local diffusion of water molecules of the nascent water fingers toward the interior of the hydrophobic core. Consequently, the probability of pore formation is lowered, increasing the electric field required to permeabilize the bilayer. It was also shown that oxidative damage to the cell plasma membrane (i.e., the presence of oxidized lipids) enhances the susceptibility of the membrane to electroporation, as such lipids are more permeable to water (206).

Comparing specifically archaeal lipids (glucosyl-myo and myo-inositol headgroups) to normal phosphatidylcholine (PC) lipids, the higher electroporation thresholds for the former were attributed (145, 146) to the strong hydrogen-bonding network that stabilizes the headgroup–headgroup interactions. In another study, the higher electroporation thresholds for phosphatidylethanolamine (PE) bilayers compared to PC bilayers (69) were linked to interlipid hydrogen bonding taking place in the PE bilayer that leads to a more densely packed water/lipid interface. Considering asymmetric bilayers composed of PC and PE lipid leaflets, the same authors observed that the pore initiation (i.e., the water column formation) is also asymmetric, with first steps taking place primarily in the PC leaflet. Studying more complex composition membranes, it was found that the membrane of the Gram-positive bacterium *Staphylococcus aureus* is less resistant to poration than the outer membrane of the Gram-negative bacterium *Escherichia coli*, with the higher electroporation threshold of the latter reflecting the reduced mobility of the lipopolysaccharide molecules located in its membrane's outer monolayer (144).

Additional factors, such as the presence of chemical agents and compounds, modify the electroporation threshold of membrane models by affecting their stability. Owing to the unusual abundance of the tryptophan amino acid in membrane proteins existing inside the membrane near the membrane/water interface, it is widely accepted that these amino acids play an important role as membrane protein anchors (43). Modeling the effect of electroporation on bilayers embedding membrane proteins, it was shown that a cyclic peptide nanotube stabilizes the bilayer in its proximity by forming strong hydrogen bonds between its tryptophan residues and the neighboring lipid headgroups, preventing pore formation in the vicinity of the channel (188). The ability of surfactants [e.g., the polyoxyethylene glycol ($C_{12}E_8$)] to lower the electroporation threshold was linked to the high mobility of such compounds and their hydrophilic moiety that affect the intrinsic properties of the host bilayer, facilitating water intrusion (147). Another MD study reported that the addition of dimethyl sulfoxide (DMSO) halves the minimum electric field required to electroporate both pure lipid and cholesterol rich bilayers (48). The authors suggested it is due to a synergy of three cofactors: (*a*) penetration of DMSO into the hydrophobic region in the lipid/water interface that decreases the lateral pressure, thus facilitating intrusion of water into the membrane; (*b*) alteration of the electrostatic membrane potential; and (*c*) release of the surface tension when the hydrophobic water pore is formed.

3.4. Transport of Solutes Across Aqueous Pores

Pores created in lipid bilayers by electric fields are highly dynamic, with size and stability strongly dependent on the TMV (22, 49, 75, 174, 187). While at present there are no experimental techniques allowing direct visualization of pores, several attempts have been made to measure their radii by monitoring the selective uptake of molecules of different sizes (e.g., propidium iodide, YO-PRO-1, bleomycin, trypan blue, PEG, sugars, and dextrans) particularly in cells, but the reliability of this approach remains questionable, as such probes can strongly interact with the lipid bilayer and perturb the pore configuration while diffusing (88, 170, 179). Moreover, the transport of molecules across cell membranes generally needs to be monitored for seconds or minutes after applying pulses, while the molecular mechanisms relating to cell membranes' permeability in such postpulse resealing steps are yet to be elucidated (106, 180, 209).

Conductance measurements might in this context provide a more sensitive and less perturbing method to characterize pores forming in the lipid bilayer. Yet, macroscopic currents in cells subject to electric fields generally report conductance through a population of many pores as well as through a variety of ion channels (214, 217). Under imposition of a constant electric current,

conductance of single pores can be monitored as well (93, 101, 103). However, accurate characterization of the pore properties from conductance measurements requires the use of a valid and reliable theoretical model, which can quantitatively predict the pore conductance. Typically, more or less simplified expressions derived from the coupled Poisson and Nernst–Planck's (PNP) equations (5, 83, 110) are used to estimate pore sizes (85, 93, 100, 101, 103). A recent review (158) of estimates from various experimental studies shows that pore sizes and conductances typically fall into the nanometer and nanosiemens (nS) ranges, respectively.

MD provides a unique method to study the transport of ions and molecules through aqueous pores in relation to the pore structure and geometry. MD simulations of simple lipid bilayers show that pore conductance depends on the pore size and the type of ions passing through the pore (22, 70, 75, 107). In bilayers subject to TMV ranging from ~400 to ~650 mV, hydrophilic pores with stable radii (1–2.5 nm) form and allow for ionic conductance in the range of 6.4 to 29.5 nS, with pores being more conductive to Cl^- than Na^+ ions (22). These results could be described quantitatively with an improved continuum model based on the PNP equations, provided that the model accounted for the binding of Na^+ ions to lipid headgroups and the electroosmotic flow induced through the pore (158).

Although a wide range of electroporation-based applications aim to transport molecules (e.g., dyes, drugs, and genetic material) across permeabilized cell membranes, little is known about the molecular mechanisms and timescale involved in these processes. Even information gathered from MD simulations to investigate such processes is scarce. Only a handful of simulations were performed to model the transport of large molecules (18, 23, 170, 188). Two such molecules, the double-stranded siRNA and Tat11, were recently investigated (23) to compare their mechanism of electric-field-mediated transport with pulse durations in the microsecond to millisecond range to those in the nanosecond range (18, 170). The electrically driven uptake of a small charged molecule such as Tat11 through an electroporated lipid bilayer occurs in tens of nanoseconds in both cases (170) and does not involve interaction with the pore. Interestingly, the simulations show that subject to either pulse type, the translocation of siRNA through lipid pores takes place in the tens of nanoseconds timescale as well. In contrast to Tat11, siRNA remains though anchored to the lipid headgroups after translocation without diffusing in the bulk solution even if the voltage is maintained.

The timescales indicated by such studies might seem puzzling, as they are orders of magnitude faster than those often reported from experimental investigations in cells, for instance. It is important, however, to note that MD studies provide only a microscopic description of the transport across the lipid bilayer component of cell membranes, while transfer, in particular of large molecules such as DNA plasmids, necessarily implies interactions with other components such as the cytoskeleton and might be modulated by more complex biological cell trafficking mechanisms (166, 167, 173).

4. MOLECULAR MECHANISMS OF LIPID BILAYER ELECTROPERMEABILIZATION

4.1. Experimental Evidence of Electric-Field-Mediated Lipid Peroxidation

Regarding the effects of chemical nature, it was reported over two decades ago that the composition and properties of both pure lipid bilayers and cell membranes can be altered by exposure to traditional electric pulses used in the electroporation technologies and treatments as a result of oxidation of their lipid constituents (11, 53, 117, 118). The fact that such exposure can cause lipid

peroxidation has been confirmed in bacteria (216, 218), plant cells (15, 117), and mammalian cells (11, 117, 118), as well as in liposomes made from polyunsaturated lipids (11, 19, 118, 219).

Studies with microsecond and millisecond pulses demonstrated that electric pulses induce generation of reactive oxygen species (ROS) and oxidative damage of unsaturated lipids, in both model and cell membranes, as confirmed by measuring the concentration of conjugated dienes, malondialdehyde (11), and hydrogen peroxide (117, 118) by using chemiluminescent probe lucigenin to detect superoxide anion radicals (53) and by analyzing the photooxidation reaction of 5-(N-hexadecanoyl)-aminofluorescein incorporated into the cell membrane (55). Results demonstrated that ROS concentration and extent of lipid peroxidation increase with electric field intensity (11, 53, 55, 117, 118), pulse duration, and number of pulses (53) and are correlated with cell membrane permeability (53, 117, 118), membrane resealing time (53), and cell damage (11, 53). Enhanced ROS generation was confirmed in submicrosecond pulse exposure as well (140).

4.2. Mechanisms of Electric-Field-Mediated Lipid Peroxidation

Lipid peroxidation typically affects unsaturated lipids bearing allylic or bis-allylic sites and takes place through a reaction chain mechanism. ROS, either generated from endogenous sources (mitochondria, plasma membrane, endoplasmic reticulum, or peroxisomes) or produced as a result of exogenous stimuli (ionizing radiation or tobacco smoke, for instance) through O_2 reduction, are among the radical species that can act as initiators of such a mechanism (2, 125, 202). Among them, the hydroxyl radical (HO•), the superoxide radical anion ($O_2^{\bullet -}$), and the hydroperoxyl radical (HOO•) are short lived and highly reactive and, therefore, are supposed to play a prominent role in cell membranes' lipid peroxidation (123). The interactions between ROS and phospholipid membranes have been studied using spin traps and fluorescent probes (16, 50, 59, 177). Classical MD simulations (33) indicate that, unlike $O_2^{\bullet -}$, both HO• and HOO• can reach peroxidation sites located along the unsaturated lipid hydrophobic chains.

It was shown that electric fields do not themselves create radicals in solution (18), in agreement with predictions from state-of-the-art quantum calculations (169), yet under electric field intensities characteristic of electroporation, electric pulses can initiate ROS production inside cells (53, 55, 140). This is consistent with recent reports that imply that submicrosecond pulses may damage cell mitochondria (9, 160). While until recently, the common view was that this radical production is sufficient to enhance the lipid membranes' peroxidation, recent experiments on giant unilamellar vesicles (GUVs) tend to show that lipid peroxidation can be promoted by ROS already present in the solution before the delivery of electric pulses (18). To date, there are yet no studies explaining the mechanisms involved behind such a behavior, and what minimal electric field is required to trigger this effect is not clear either.

4.3. Stability and Permeability of Peroxidized Bilayers

Hydroperoxides (i.e., the primary lipid peroxidation products) are stable enough to persist and diffuse in lipid bilayers. It was recently shown (159) that the permeability and conductance of lipid bilayers to ions increase by several orders of magnitude with increasing content of peroxidized lipids. Hydroperoxide lipid derivatives are, however, also prone to secondary degradation, resulting in various products with truncated lipid tails ending with either an aldehyde or carboxylic group (80). Fluorescence, electron paramagnetic resonance, and MD studies indicate that the presence of oxidized lipids decreases the lipid order, lowers the phase transition temperature, leads to lateral expansion and thinning of the bilayer, increases lipid mobility and augments flip-flop, influences lateral phase organization, promotes formation of water defects, and under extreme conditions

leads to disintegration of the bilayer (79, 80, 212). Oxidized lipids are by far more permeable than their nonoxidized counterparts and are prone to spontaneous pore formation. The presence of oxidized lipids with an aldehyde group disturbs the bilayer more than the presence of ones with a peroxide group does (17) and enhances the membrane susceptibility to electric-field-mediated pore formation (206). Of particular note, membranes with significant aldehyde group content can ultimately undergo spontaneous pore formation (17, 37, 113, 203), a scenario not present in lipids containing the peroxide group (17, 203).

4.4. Functional Consequences of Oxidatively Damaged Membranes

The contribution of lipid peroxidation to the permeability of electropermeabilized cell membranes has not yet been quantitatively assessed. This is a challenging task that requires characterization of the type and amount of lipid oxidation products in electropermeabilized cell membranes, as well as the quantification of the permeability of the peroxidized parts of the membrane. A recent study (159) estimated the permeability and conductance of bilayer patches containing hydroperoxide lipid derivatives and compared them to experimental measurements on electropermeabilized cells. Their analysis indicates that the permeability and conductance of hydroperoxide lipid derivatives are sufficient to account for the lowest measured values but not high enough to reasonably explain the entire range of experimental measurements. However, oxidatively damaged membrane lesions that contain secondary lipid oxidative products could, as stated above, exhibit spontaneous pore formation and might relate to higher values of postpulse permeability and conductance as measured in electropermeabilized cell membranes, but further modeling studies are required to quantify such a permeability.

5. FROM SIMPLE LIPID BILAYERS TO THE COMPLEX STRUCTURE OF THE CELL MEMBRANE

The main players in electropermeabilization are considered to be membrane lipids. Thus, a large part of the understanding of basic electropermeabilization mechanisms has been gained through experiments on model lipid systems, including planar lipid bilayers (1, 12, 13) and lipid vesicles (84, 129, 148, 161, 192). Particularly, GUVs, which most closely mimic the size and curvature of the cell membrane, have become popular models for studying electropermeabilization (45, 143, 149, 161). However, the response of a GUV to permeabilizing electric pulses differs markedly from that of a cell; specifically, the Maxwell stress induces large electrodeformation of the GUV membrane, which can be accompanied by creation of micrometer-sized pores (macropores) and expulsion of lipids from the GUV (148, 161). These differences in response show that GUVs are oversimplified cell models. Indeed, evidence is building that membrane proteins and the cytoskeleton network contribute importantly to cell membrane electropermeabilization, as we review in Sections 5.1 and 5.2, respectively.

5.1. Effects of the Electric Field on Membrane Proteins

The first report that membrane electropermeabilization can be partly attributed to the effect on membrane proteins dates to 1980, when it was observed that in low-conductivity media, exposure of erythrocytes to pulses inducing lipid bilayer electropermeabilization also increased the electric conductivity of transmembrane Na^+/K^+-ATPases, albeit this effect was not detectable at physiological levels of medium conductivity (191). Ten years later, this was formulated into a coherent hypothesis of denaturation of transmembrane transport proteins owing to TMV-driven

supraphysiological current passing through them during the exposure to electric pulses and the resulting local heating (200, 201). It was also estimated that electropermeabilization-inducing pulses can generate sufficient heating for denaturation and that subsequent excision of denatured proteins from the membrane—and thus recovery of its impermeable state—requires minutes to tens of minutes (200, 201).

Experimental progress in this field required utilization of advanced patch-clamp techniques, which confirmed that electropermeabilization-inducing pulses, particularly with submicrosecond durations and correspondingly high amplitudes, can affect the conductivity of transmembrane protein structures, including K^+ channels (28) and voltage-gated Ca^{2+} and Na^+ channels (20, 29, 130, 131, 138, 214). Still, while a potentiating effect was observed for some structures and pulse parameters, resulting in an increased and/or prolonged transmembrane conductivity of these structures, for other structures, pulse parameters, and/or experimental conditions, an inhibiting effect was found, resulting in a decreased conductivity (29, 130, 131, 191). Furthermore, the effect on Ca^{2+} channels was observed to be direction dependent, with differing conductivities for inward and outward flow of Ca^{2+} ions (214). The effect of electropermeabilization-inducing pulses on voltage-gated Ca^{2+} channels was also observed by fluorescence microscopy (34), while confocal Raman microspectroscopy was recently used to demonstrate accompanying changes in vibrational modes of specific amino acids in cellular proteins (3, 4), albeit this method did not allow differentiating between signals from membrane-bound and cytoplasmic proteins. As a complement to these experimental studies, an MD simulation has been utilized to study the effects of electropermeabilization-inducing pulses on transmembrane water channels (aquaporins), finding a significant effect on water self-diffusion during and immediately after the pulses (155).

5.2. Effects of the Electric Field on Cytoskeleton Components

The earliest indications that the integrity of the cytoskeleton and the intensity of electropermeabilization are related were reported in 1992 (164), but this study and two subsequent ones focused on the effect of cytoskeleton modification—achieved either chemically (127, 164) or physically (128)—on subsequent electropermeabilization, finding that both its extent and duration are affected by such modification. The investigators started to focus on the effect of electropermeabilization itself on cytoskeleton integrity only a decade later, revealing that both F-actin and β-tubulin proteins in the cytoskeleton are disrupted by electropermeabilization-inducing pulses and that the cytoskeleton recovery becomes detectable within hours (87, 121). Soon after, such cytoskeleton disruption was analyzed by atomic force microscopy, which revealed up to a 40% decrease in membrane stiffness (31), accompanied by membrane rippling, cell swelling, and destabilization of F-actin in the cell cortex underlying the plasma membrane followed by cytoskeleton recovery within hours (30, 31). The second of these studies also suggested that the main effect of electric pulses on cortical actin is not its depolymerization but rather its impaired attachment to the membrane (30), which was already reported earlier for much longer exposures of cells to direct electric fields far too weak to induce electropermeabilization (197).

Yet a crucial question that remained open was whether the cytoskeleton integrity is disrupted directly by the electric pulses or indirectly owing to the resulting electropermeabilization. Namely, electropermeabilization results in ATP leakage (163) and thus depletes the intracellular ATP crucial for sustaining actin polymerization (91), but as described above, some experiments suggest that depolymerization of cortical actin is, at most, of secondary importance compared to the cortex detachment from the membrane (30). Furthermore, electropermeabilization often results in cell swelling due to osmotic and/or ionic imbalances (201), and such swelling can disrupt the cytoskeleton (72), yet conversely, cytoskeleton disruption can also lead to cell swelling (142). The situation is even more complex with submicrosecond pulses, which were also shown to induce

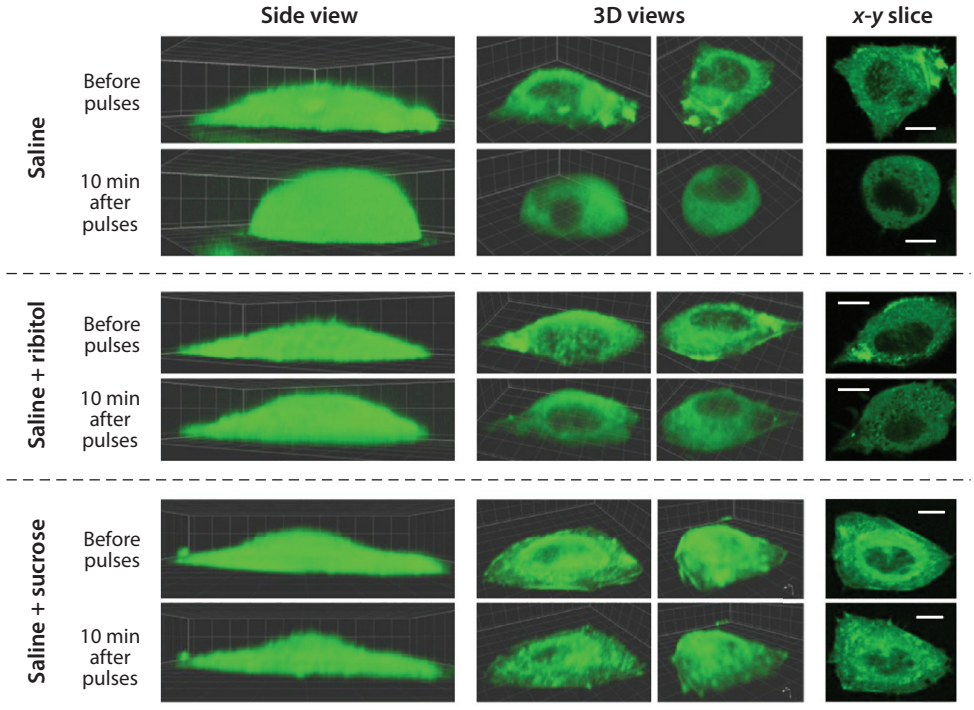

Figure 5

Cell swelling and actin cytoskeleton disruption caused by electropermeabilization of Chinese hamster ovary cells with four 600-ns, 19.2-kV/cm pulses delivered with a 0.5-s period. (*Top*) In physiological saline, swelling is pronounced, as is loss of actin structure. (*Middle*) In physiological saline supplemented with ribitol, swelling is limited, but loss of actin structure is still clearly visible. (*Bottom*) In physiological saline supplemented with sucrose, swelling is blocked and actin structure remains intact, implying that disruption of actin cytoskeleton is a downstream effect of cell swelling, which is in turn the effect of electropermeabilization. In the side views and 3D views, the grid size is 5 × 5 μm, while in the *x-y* slices, the bar corresponds to 10 μm. Figure adapted from Reference 139 with permission.

both cell swelling and cytoskeleton disruption (183, 213), but as such pulses can also permeabilize intracellular organelles (8), the effect on the cytoskeleton could also result from release of intraorganelle enzymes (e.g., caspases) and ions (particularly Ca^{2+}) into the cytosol. In 2014, it was shown rather conclusively that—at least with the electropermeabilization protocol applied, namely four 600-ns 19.2-kV/cm pulses delivered with a 0.5-s period—disruption of the actin cytoskeleton is a result of cell swelling and not vice versa (139); the decisive experiment is summarized in **Figure 5**. Still, at least three studies performed with different pulse parameters suggested actin disruption can occur also without cell swelling, with two reporting this with even shorter and more intense (10 ns, 33 kV/cm) pulses (14, 76) and one with much longer and weaker (100 μs, up to 200 V/cm) pulses (87). Thus, the question of whether electropermeabilization-inducing pulses can disrupt the cytoskeleton only indirectly or also directly is not yet generally settled in a conclusive manner.

6. REMAINING CHALLENGES

The mechanisms of electropermeabilization have been investigated for at least four decades, yet there are still open questions remaining to be answered. One of the main reasons why

understanding electropermeabilization is challenging is the wide range of length scales (from nanometers-thick membrane through micrometers-large cells up to centimeters-large tissue segments) and timescales involved (from nanoseconds to hours, as described in **Table 1**). Thus, investigation of electropermeabilization requires a multi-scale modeling approach, ranging from molecular simulations to large-scale continuum models of cells and tissues, closely coupled with systematic experiments. In recent years, such an approach has indeed resulted in significant progress, as outlined in this review.

Nevertheless, one of the remaining issues that many modelers experience is the lack of quantitative experimental data to which the modeling results can be compared. For instance, experimental measurements cannot directly discriminate between the molecular transport through pores and that through the oxidized parts of the membrane. Still, with today's computational resources, one can quantify this transport via MD simulations, and by comparing it quantitatively to the measured transport, one can predict the number of pores or the area of oxidized lesions. These predictions can be further compared to predictions from continuum electropermeabilization models to test the validity of the models and the hypotheses on which they are built. The importance of transport quantification, in terms of both the number of transported solutes into the cell and its time course, is increasingly being recognized (137, 179–180).

While there is a general consensus that the TMV induced by an electric field promotes formation of pores in the lipid bilayer, the contribution of other mechanisms to cell membrane electropermeabilization, including oxidative membrane damage and conformational changes of membrane proteins, remains to be elucidated. The long-standing assumption that the pores formed during the pulse are also the main transport mechanism for seconds and minutes after the pulse (38, 64, 176, 178) is now questioned, as MD simulations show no evidence of pores retaining their (meta)stability once TMV vanishes or drops to a very low level. A plausible hypothesis is that these primary pores evolve into more complex pores involving both lipidic and other molecules, but the molecular organization of these putative complex pores is yet unknown (208). Another possibility is that the electric-field-mediated lipid oxidation results in spontaneous formation of pores in oxidized membrane lesions. Both imply that we may need to distinguish between at least two different types of pores; this has already been proposed before (134, 141), but a description of the underlying pore structure has yet to be provided. Still another possibility is that the long-lived permeability after the pulse does not involve pores at all but instead is mediated by leaky peroxidized membrane lesions and/or modified membrane proteins (189).

It also remains to be fully elucidated how the cell response to the electric stimulus contributes to electropermeabilization. There is experimental evidence suggesting that cell membrane repair mechanisms are involved in membrane resealing (32, 77). To separate the downstream effects of the cell response to the electric field exposure from direct effects of the electric field on its membrane, it is important to systematically study biomimetic systems. In addition, bottom-up studies on biomimetic systems such as GUVs could help determine the role of individual cell structures on electropermeabilization. It has already been shown that the presence of agarose meshwork inside the GUV (emulating the highly viscous and crowded cytoplasm) can obstruct the created pores and keep the membrane highly permeable (112). Additional studies on GUVs with increasing complexity, such as incorporation of membrane proteins and cytoskeleton network, should further improve the understanding of these structures' role in electropermeabilization.

Answering the above questions is a prerequisite for optimization of existing and development of new electroporation-based treatments, including cancer treatment by electrochemotherapy or irreversible electroporation (60, 61, 119, 171, 215), cardiac tissue ablation (185, 210), and DNA vaccination (105). Until now, excitable cells and tissues were not the focus of electroporation research but whether they respond to electropermeabilizing pulses similarly to nonexcitable cells,

either as target tissue or as collateral damage, is becoming increasingly important to understand. Either targeting or avoiding damage to nerves, brain, cardiac tissue (for defibrillation), and muscle (as a DNA vaccination target), to name a few applications, will require these answers.

Even in preparing this review, we were facing difficulties in summarizing the existing findings, as experimental detail is lacking in many reports, making comparison of results from different studies difficult if not impossible. To address this, it would be extremely important for further studies to follow recently published recommendations (25, 154)—in particular, evaluating the local electric field, often estimated as the voltage-to-distance ratio, despite diverse electrode geometries for many of which such estimation is an oversimplification.

DISCLOSURE STATEMENT

D.M. is the inventor of several patents pending and granted, is receiving royalties, and is consulting for different companies and organizations that are active in the area of electroporation and electroporation-based technologies and therapies while his research team is engaged in sponsored research.

ACKNOWLEDGMENTS

Part of this research was supported under various grants from the Slovenian Research Agency (ARRS) and French National Center for Scientific Research (CNRS), and conducted within the scope of the European Laboratory of Pulsed Electric Fields Applications in Biology and Medicine (LEA EBAM). M.T. also acknowledges the support from the Contrat État Plan Region Lorraine 2015–2020 subproject MatDS.

LITERATURE CITED

1. Abidor IG, Arakelyan VB, Chernomordik LV, Chizmadzhev YA, Pastushenko VF, Tarasevich MR. 1979. Electric breakdown of bilayer membranes: I. The main experimental facts and their qualitative discussion. *Bioelectrochem. Bioenerg.* 6:37–52
2. Ayala A, Muñoz MF, Argüelles S. 2014. Lipid peroxidation: production, metabolism, and signaling mechanisms of malondialdehyde and 4-hydroxy-2-nonenal. *Oxid. Med. Cell. Longev.* 2014:360438
3. Azan A, Untereiner V, Descamps L, Merla C, Gobinet C, et al. 2017. Comprehensive characterization of the interaction between pulsed electric fields and live cells by confocal Raman microspectroscopy. *Anal. Chem.* 89:10790–97
4. Azan A, Untereiner V, Gobinet C, Sockalingum GD, Breton M, et al. 2017. Demonstration of the protein involvement in cell electropermeabilization using confocal Raman microspectroscopy. *Sci. Rep.* 7:40448
5. Barnett A. 1990. The current-voltage relation of an aqueous pore in a lipid bilayer membrane. *Biochim. Biophys. Acta* 1025:10–14
6. Barnett A, Weaver JC. 1991. Electroporation: a unified, quantitative theory of reversible electrical breakdown and rupture. *Bioelectrochem. Bioenerg.* 25:163–82
7. Batista Napotnik T, Reberšek M, Kotnik T, Lebrasseur E, Cabodevila G, Miklavčič D. 2010. Electropermeabilization of endocytotic vesicles in B16 F1 mouse melanoma cells. *Med. Biol. Eng. Comput.* 48:407–13
8. Batista Napotnik T, Reberšek M, Vernier PT, Mali B, Miklavčič D. 2016. Effects of high voltage nanosecond electric pulses on eukaryotic cells (in vitro): a systematic review. *Bioelectrochemistry* 110:1–12
9. Batista Napotnik T, Wu YH, Gundersen AM, Miklavčič D, Vernier PT. 2012. Nanosecond electric pulses cause mitochondrial membrane permeabilization in Jurkat cells. *Bioelectromagnetics* 33:257–64
10. Bennett WFD, Sapay N, Tieleman DP. 2014. Atomistic simulations of pore formation and closure in lipid bilayers. *Biophys. J.* 106:210–19

11. Benov LC, Antonov PA, Ribarov SR. 1994. Oxidative damage of the membrane lipids after electroporation. *Gen. Physiol. Biophys.* 13:85–97
12. Benz R, Beckers F, Zimmermann U. 1979. Reversible electrical breakdown of lipid bilayer membranes: a charge-pulse relaxation study. *J. Membrane Biol.* 48:181–204
13. Benz R, Zimmermann U. 1981. The resealing process of lipid bilayers after reversible electrical breakdown. *Biochim. Biophys. Acta* 640:169–78
14. Berghofer T, Eing C, Flickinger B, Hohenberger P, Wegner LH, et al. 2009. Nanosecond electric pulses trigger actin responses in plant cells. *Biochem. Biophys. Res. Commun.* 387:590–95
15. Biedinger U, Youngman RJ, Schnabl H. 1990. Differential effects of electrofusion and electropermeabilization parameters on the membrane integrity of plant protoplasts. *Planta* 180:598–602
16. Bodner E, Afri M, Frimer AA. 2010. Determining radical penetration into membranes using ESR splitting constants. *Free Radic. Biol. Med.* 49:427–36
17. Boonnoy P, Jarerattanachat V, Karttunen M, Wong-Ekkabut J. 2015. Bilayer deformation, pores, and micellation induced by oxidized lipids. *J. Phys. Chem. Lett.* 6:4884–88
18. Breton M, Delemotte L, Silve A, Mir LM, Tarek M. 2012. Transport of siRNA through lipid membranes driven by nanosecond electric pulses: an experimental and computational study. *J. Am. Chem. Soc.* 134:13938–41
19. Breton M, Mir LM. 2018. Investigation of the chemical mechanisms involved in the electropulsation of membranes at the molecular level. *Bioelectrochemistry* 119:76–83
20. Burke RC, Bardet SM, Carr L, Romanenko S, Arnaud-Cormos D, et al. 2017. Nanosecond pulsed electric fields depolarize transmembrane potential via voltage-gated K^+, Ca^{2+} and TRPM8 channels in U87 glioblastoma cells. *Biochim. Biophys. Acta* 1859:2040–50
21. Casciola M, Bonhenry D, Liberti M, Apollonio F, Tarek M. 2014. A molecular dynamic study of cholesterol rich lipid membranes: comparison of electroporation protocols. *Bioelectrochemistry* 100:11–17
22. Casciola M, Kasimova MA, Rems L, Zullino S, Apollonio F, Tarek M. 2016. Properties of lipid electropores I: molecular dynamics simulations of stabilized pores by constant charge imbalance. *Bioelectrochemistry* 109:108–16
23. Casciola M, Tarek M. 2016. A molecular insight into the electro-transfer of small molecules through electropores driven by electric fields. *Biochim. Biophys. Acta* 1858:2278–89
24. Čemažar M, Jarm T, Miklavčič D, Maček-Lebar A, Ihan A, et al. 1998. Effect of electric-field intensity on electropermeabilization and electrosensitmty of various tumor-cell lines in vitro. *Electro- Magnetobiol.* 17:263–72
25. Čemažar M, Serša G, Frey W, Miklavčič D, Teissié J. 2018. Recommendations and requirements for reporting on applications of electric pulse delivery for electroporation of biological samples. *Bioelectrochemistry* 122:69–76
26. Chang DC, Reese TS. 1990. Changes of membrane structure induced by electroporation as revealed by rapid-freezing electron microscopy. *Biophys. J.* 58:1–12
27. Chen N, Schoenbach KH, Kolb JF, Swanson RJ, Garner AL, et al. 2004. Leukemic cell intracellular responses to nanosecond electric pulses. *Biochem. Biophys. Res. Commun.* 317:421–42
28. Chen W, Han Y, Chen Y, Astumian D. 1998. Electric field-induced functional reductions in the K^+ channels mainly resulted from supramembrane potential-mediated electroconformational changes. *Biophys. J.* 75:196–206
29. Chen W, Zhongsheng Z, Lee RC. 2006. Supramembrane potential-induced electroconformational changes in sodium channel proteins: a potential mechanism involved in electric injury. *Burns* 32:52–59
30. Chopinet L, Dague E, Rols MP. 2014. AFM sensing cortical actin cytoskeleton destabilization during plasma membrane electropermeabilization. *Cytoskeleton* 71:587–94
31. Chopinet L, Roduit C, Rols MP, Dague E. 2013. Destabilization induced by electropermeabilization analyzed by atomic force microscopy. *Biochim. Biophys. Acta* 1828:2223–29
32. Ciobanu F, Golzio M, Kovacs E, Teissié J. 2018. Control by low levels of calcium of mammalian cell membrane electropermeabilization. *J. Membrane Biol.* 251:221–28
33. Cordeiro RM. 2014. Reactive oxygen species at phospholipid bilayers: distribution, mobility and permeation. *Biochim. Biophys. Acta* 1838:438–44

34. Craviso GL, Choe S, Chatterjee P, Chatterjee I, Vernier PT. 2010. Nanosecond electric pulses: a novel stimulus for triggering Ca^{2+} influx into chromaffin cells via voltage-gated Ca^{2+} channels. *Cell. Mol. Neurobiol.* 30:1259–65
35. Crowley JM. 1973. Electrical breakdown of bimolecular lipid membranes as an electro-mechanical instability. *Biophys. J.* 13:711–24
36. Cruzeiro-Hansson L, Mouritsen OG. 1988. Passive ion permeability of lipid membranes modelled via lipid-domain interfacial area. *Biochim. Biophys. Acta* 944:63–72
37. Cwiklik L, Jungwirth P. 2010. Massive oxidation of phospholipid membranes leads to pore creation and bilayer disintegration. *Chem. Phys. Lett.* 486:99–103
38. DeBruin K, Krassowska W. 1999. Modeling electroporation in a single cell. I. Effects of field strength and rest potential. *Biophys. J.* 77:1213–24
39. Dehez F, Delemotte L, Kramar P, Miklavčič D, Tarek M. 2014. Evidence of conducting hydrophobic nanopores across membranes in response to an electric field. *J. Phys. Chem. C* 118:6752–57
40. Delemotte L, Dehez F, Treptow W, Tarek M. 2008. Modeling membranes under a transmembrane potential. *J. Phys. Chem. B* 112:5547–50
41. Delemotte L, Tarek M. 2012. Molecular dynamics simulations of lipid membrane electroporation. *J. Membrane Biol.* 245:531–43
42. Deng P, Lee YK, Lin R, Zhang TY. 2012. Nonlinear electro-mechanobiological behavior of cell membrane during electroporation. *Appl. Phys. Lett.* 101:053702
43. de Jesus AJ, Allen TW. 2013. The role of tryptophan side chains in membrane protein anchoring and hydrophobic mismatch. *Biochim. Biophys. Acta* 1828:864–76
44. Dimitrov DS. 1984. Electric field-induced breakdown of lipid bilayer and cell membranes: a thin viscoelastic film model. *J. Membr. Biol.* 78:53–60
45. Dimova R, Riske KA, Aranda S, Bezlyepkina N, Knorr RL, Lipowsky R. 2007. Giant vesicles in electric fields. *Soft Matter* 3:817–27
46. Ehrenberg B, Farkas DL, Fluhler EN, Lojewska Z, Loew LM. 1987. Membrane potential induced by external electric field pulses can be followed with a potentiometric dye. *Biophys. J.* 51:833–37
47. Fernández ML, Marshall G, Sagués F, Reigada R. 2010. Structural and kinetic molecular dynamics study of electroporation in cholesterol-containing bilayers. *J. Phys. Chem. B* 114:6855–65
48. Fernández ML, Reigada R. 2014. Effects of dimethyl sulfoxide on lipid membrane electroporation. *J. Phys. Chem. B* 118:9306–12
49. Fernández ML, Risk M, Reigada R, Vernier PT. 2012. Size-controlled nanopores in lipid membranes with stabilizing electric fields. *Biochem. Biophys. Res. Commun.* 423:325–30
50. Fortier CA, Guan B, Cole RB, Tarr MA. 2009. Covalently bound fluorescent probes as reporters for hydroxyl radical penetration into liposomal membranes. *Free Radic. Biol. Med.* 46:1376–85
51. Freeman SA, Wang MA, Weaver JC. 1994. Theory of electroporation for a planar bilayer membrane: predictions of the fractional aqueous area, change in capacitance and pore-pore separation. *Biophys. J.* 67:42–56
52. Frey W, White JA, Price RO, Blackmore PF, Joshi RP, et al. 2006. Plasma membrane voltage changes during nanosecond pulsed electric field exposure. *Biophys. J.* 90:3608–15
53. Gabriel B, Teissié J. 1994. Generation of reactive-oxygen species induced by electropermeabilization of Chinese hamster ovary cells and their consequence on cell viability. *Eur. J. Biochem.* 223:25–33
54. Gabriel B, Teissié J. 1995. Control by electrical parameters of short- and long-term cell death resulting from electropermeabilization of Chinese hamster ovary cells. *Biochim. Biophys. Acta* 1266:171–78
55. Gabriel B, Teissié J. 1995. Spatial compartmentation and time resolution of photooxidation of a cell membrane probe in electropermeabilized Chinese hamster ovary cells. *Eur. J. Biochem.* 228:710–18
56. Gabriel B, Teissié J. 1997. Direct observation in the millisecond time range of fluorescent molecule asymmetrical interaction with the electropermeabilized cell membrane. *Biophys. J.* 73:2630–37
57. Gabriel B, Teissié J. 1998. Mammalian cell electropermeabilization as revealed by millisecond imaging of fluorescence changes of ethidium bromide in interaction with the membrane. *Bioelectrochem. Bioenerg.* 47:113–18

58. Gabriel B, Teissié J. 1999. Time courses of mammalian cell electropermeabilization observed by millisecond imaging of membrane property changes during the pulse. *Biophys. J.* 76:2158–65
59. Gamliel A, Afri M, Frimer AA. 2008. Determining radical penetration of lipid bilayers with new lipophilic spin traps. *Free Radic. Biol. Med.* 44:1394–405
60. Garcia PA, Kos B, Rossmeisl JH Jr., Pavliha D, Miklavčič D. 2017. Predictive therapeutic planning for irreversible electroporation treatment of spontaneous malignant glioma. *Med. Phys.* 44:4968–80
61. Gasbarrini A, Campos WK, Campanacci L, Boriani S. 2015. Electrochemotherapy to metastatic spinal melanoma: a novel treatment of spinal metastasis? *Spine* 40:E1340–46
62. Gascoyne PRC, Pethig R, Burt JPH, Becker FF. 1993. Membrane changes accompanying the induced differentiation of Friend murine erythroleukemia cells studied by dielectrophoresis. *Biochim. Biophys. Acta* 1146:119–26
63. Gennis RB. 1989. *Biomembranes: Molecular Structure and Function*. New York: Springer
64. Glaser RW, Leikin SL, Chernomordik LV, Pastushenko VF, Sokirko AI. 1988. Reversible electrical breakdown of lipid bilayers: formation and evolution of pores. *Biochim. Biophys. Acta* 940:275–87
65. Golberg A, Sack M, Teissie J, Pataro G, Pliquett U, et al. 2016. Energy-efficient biomass processing with pulsed electric fields for bioeconomy and sustainable development. *Biotechnol. Biofuels* 9:94
66. Golzio M, Mora MP, Raynaud C, Delteil C, Teissié J, Rols MP. 1998. Control by osmotic pressure of voltage-induced permeabilization and gene transfer in mammalian cells. *Biophys. J.* 74:3015–22
67. Golzio M, Teissié J, Rols MP. 2002. Direct visualization at the single-cell level of electrically mediated gene delivery. *PNAS* 99:1292–97
68. Gumbart J, Khalili-Araghi F, Sotomayor M, Roux B. 2012. Constant electric field simulations of the membrane potential illustrated with simple systems. *Biochim. Biophys. Acta* 1818:294–302
69. Gurtovenko AA, Lyulina AS. 2014. Electroporation of asymmetric phospholipid membranes. *J. Phys. Chem. B* 118:9909–18
70. Gurtovenko AA, Vattulainen I. 2007. Ion leakage through transient water pores in protein-free lipid membranes driven by transmembrane ionic charge imbalance. *Biophys. J.* 92:1878–90
71. Henslee BE, Morss A, Hu X, Lafyatis GP, Lee LJ. 2011. Electroporation dependence on cell size: optical tweezers study. *Anal. Chem.* 83:3998–4003
72. Henson JH. 1999. Relationships between the actin cytoskeleton and cell volume regulation. *Microsc. Res. Tech.* 47:155–62
73. Hibino M, Itoh H, Kinosita K Jr. 1993. Time courses of cell electroporation as revealed by submicrosecond imaging of transmembrane potential. *Biophys. J.* 64:1789–1800
74. Hibino M, Shigemori M, Itoh H, Nagayama K, Kinosita K Jr. 1991. Membrane conductance of an electroporated cell analyzed by submicrosecond imaging of transmembrane potential. *Biophys. J.* 59:209–20
75. Ho MC, Casciola M, Levine ZA, Vernier PT. 2013. Molecular dynamics simulations of ion conductance in field-stabilized nanoscale lipid electropores. *J. Phys. Chem. B* 117:11633–40
76. Hohenberger P, Eing C, Straessner R, Durst S, Frey W, Nick P. 2011. Plant actin controls membrane permeability. *Biochim. Biophys. Acta* 1808:2304–12
77. Huynh C, Roth D, Ward DM, Kaplan J, Andrews NW. 2004. Defective lysosomal exocytosis and plasma membrane repair in Chediak-Higashi/beige cells. *PNAS* 101:16795–800
78. Israelachvili JN, Pashley RM. 1984. Measurement of the hydrophobic interaction between two hydrophobic surfaces in aqueous electrolyte solutions. *J. Coll. Interface Sci.* 98:500–14
79. Jarerattanachat V, Karttunen M, Wong-Ekkabut J. 2013. Molecular dynamics study of oxidized lipid bilayers in NaCl solution. *J. Phys. Chem. B* 117:8490–501
80. Jurkiewicz P, Olżyńska A, Cwiklik L, Conte E, Jungwirth P, et al. 2012. Biophysics of lipid bilayers containing oxidatively modified phospholipids: insights from fluorescence and EPR experiments and from MD simulations. *Biochim. Biophys. Acta* 1818:2388–402
81. Kakorin S, Brinkmann U, Neumann E. 2005. Cholesterol reduces membrane electroporation and electric deformation of small bilayer vesicles. *Biophys. Chem.* 117:155–71
82. Kakorin S, Liese T, Neumann E. 2003. Membrane curvature and high-field electroporation of lipid bilayer vesicles. *J. Phys. Chem. B* 107:10243–51

83. Kakorin S, Neumann E. 2002. Ionic conductivity of electroporated lipid bilayer membranes. *Bioelectrochemistry* 56:163–66
84. Kakorin S, Stoylov SP, Neumann E. 1996. Electro-optics of membrane electroporation in diphenylhexatriene-doped lipid bilayer vesicles. *Biophys. Chem.* 58:109–16
85. Kalinowski S, Ibron G, Bryl K, Figaszewski Z. 1998. Chronopotentiometric studies of electroporation of bilayer lipid membranes. *Biochim. Biophys. Acta* 1369:204–12
86. Kandušer M, Šentjurc M, Miklavčič D. 2008. The temperature effect during pulse application on cell membrane fluidity and permeabilization. *Bioelectrochemistry* 74:52–57
87. Kanthou C, Kranjc S, Serša G, Tozer G, Zupanič A, Čemažar M. 2006. The endothelial cytoskeleton as a target of electroporation-based therapies. *Mol. Cancer Ther.* 5:3145–52
88. Kapla J, Wohlert J, Stevensson B, Engström O, Widmalm G, Maliniak A. 2013. Molecular dynamics simulations of membrane–sugar interactions. *J. Phys. Chem. B* 117:6667–73
89. Kennedy SM, Ji Z, Hedstrom JC, Booske JH, Hagness SC. 2008. Quantification of electroporative uptake kinetics and electric field heterogeneity effects in cells. *Biophys. J.* 94:5018–27
90. Kirsch SA, Böckmann RA. 2016. Membrane pore formation in atomistic and coarse-grained simulations. *Biochim. Biophys. Acta* 1858:2266–77
91. Korn ED, Carlier MF, Pantaloni D. 1987. Actin polymerization and ATP hydrolysis. *Science* 238:638–44
92. Koronkiewicz S, Kalinowski S. 2004. Influence of cholesterol on electroporation of bilayer lipid membranes: chronopotentiometric studies. *Biochim. Biophys. Acta* 1661:196–203
93. Koronkiewicz S, Kalinowski S, Bryl K. 2002. Programmable chronopotentiometry as a tool for the study of electroporation and resealing of pores in bilayer lipid membranes. *Biochim. Biophys Acta* 1561:222–29
94. Kotnik T, Frey W, Sack M, Haberl Meglič S, Peterka M, Miklavčič D. 2015. Electroporation-based applications in biotechnology. *Trends Biotechnol.* 33:480–88
95. Kotnik T, Maček Lebar A, Miklavčič D, Mir LM. 2000. Evaluation of cell membrane electropermeabilization by means of nonpermeant cytotoxic agent. *Biotechniques* 28:921–26
96. Kotnik T, Miklavčič D. 2000. Second-order model of membrane electric field induced by alternating external electric fields. *IEEE Trans. Biomed. Eng.* 47:1074–81
97. Kotnik T, Miklavčič D. 2006. Theoretical evaluation of voltage inducement on internal membranes of biological cells exposed to electric fields. *Biophys. J.* 90:480–91
98. Kotnik T, Miklavčič D, Slivnik T. 1998. Time course of transmembrane voltage induced by time-varying electric fields—a method for theoretical analysis and its application. *Bioelectrochem. Bioenerg.* 45:3–16
99. Kotnik T, Pucihar G, Miklavčič D. 2010. Induced transmembrane transport and its correlation with electroporation-mediated molecular transport. *J. Membrane Biol.* 236:3–13
100. Kotulska M, Basalyga J, Derylo MB, Sadowski P. 2010. Meta-stable pores at the onset of constant-current electroporation. *J. Membr. Biol.* 236:37–41
101. Kramar P, Delemotte L, Maček Lebar A, Kotulska M, Tarek M, Miklavčič D. 2012. Molecular-level characterization of lipid membrane electroporation using linearly rising current. *J. Membrane Biol.* 245:651–59
102. Kramar P, Miklavčič D, Maček Lebar A. 2009. A system for the determination of planar lipid bilayer breakdown voltage and its applications. *IEEE Trans. Nanobiosci.* 8:132–38
103. Krassen H, Pliquett U, Neumann E. 2007. Nonlinear current-voltage relationship of the plasma membrane of single CHO cells. *Bioelectrochemistry* 70:71–77
104. Krassowska W, Filev PD. 2007. Modeling electroporation in a single cell. *Biophys. J.* 92:404–17
105. Lambricht L, Lopes A, Kos S, Serša G, Préat V, Vandermeulen G. 2016. Clinical potential of electroporation for gene therapy and DNA vaccine delivery. *Expert Opin. Drug Deliv.* 13:295–310
106. Leguèbe M, Silve A, Mir LM, Poignard C. 2014. Conducting and permeable states of cell membrane submitted to high voltage pulses: mathematical and numerical studies validated by the experiments. *J. Theor. Biol.* 360:83–94
107. Leontiadou H, Mark AE, Marrink SJ. 2007. Ion transport across transmembrane pores. *Biophys. J.* 92:4209–15
108. Levine ZA, Vernier PT. 2010. Life cycle of an electropore: field-dependent and field-independent steps in pore creation and annihilation. *J. Membrane Biol.* 236:27–36

109. Levine ZA, Vernier PT. 2012. Calcium and phosphatidylserine inhibit lipid electropore formation and reduce pore lifetime. *J. Membrane Biol.* 245:599–610
110. Li J, Lin H. 2010. The current-voltage relation for electropores with conductivity gradients. *Biomicrofluidics* 4:013206
111. Li J, Lin H. 2011. Numerical simulation of molecular uptake via electroporation. *Bioelectrochemistry* 82:10–21
112. Lira RB, Dimova R, Riske KA. 2014. Giant unilamellar vesicles formed by hybrid films of agarose and lipids display altered mechanical properties. *Biophys. J.* 107:1609–19
113. Lis M, Wizert A, Przybylo M, Langner M, Swiatek J, et al. 2011. The effect of lipid oxidation on the water permeability of phospholipids bilayers. *Phys. Chem. Chem. Phys.* 13:17555–63
114. Litster JD. 1975. Stability of lipid bilayers and red blood cell membranes. *Phys. Lett.* 53A:193–94
115. Lopez A, Rols MP, Teissie J. 1988. ^{31}P NMR analysis of membrane phospholipid organization in viable, reversibly electropermeabilized Chinese hamster ovary cells. *Biochemistry* 27:1222–28
116. Lyon DY, Pivetal J, Blanchard L, Vogel TM. 2010. Bioremediation via in situ electrotransformation. *Bioremediat. J.* 14:109–19
117. Maccarrone M, Bladergroen MR, Rosato N, Agro AF. 1995. Role of lipid peroxidation in electroporation-induced cell permeability. *Biochem. Biophys. Res. Commun.* 209:417–25
118. Maccarrone M, Rosato N, Agro AF. 1995. Electroporation enhances cell membrane peroxidation and luminescence. *Biochem. Biophys. Res. Commun.* 206:238–45
119. Mali B, Jarm T, Snoj M, Serša G, Miklavčič D. 2013. Antitumor effectiveness of electrochemotherapy: a systematic review and meta-analysis. *Eur. J. Surg. Oncol.* 39:4–16
120. Melikov KC, Frolov VA, Shcherbakov A, Samsonov AV, Chizmadzhev YA, Chernomordik LV. 2001. Voltage-induced nonconductive pre-pores and metastable single pores in unmodified planar lipid bilayer. *Biophys. J.* 80:1829–36
121. Meulenberg CJW, Todorović V, Čemažar M. 2012. Differential cellular effects of electroporation and electrochemotherapy in monolayers of human microvascular endothelial cells. *PLOS ONE* 7(12):e52713
122. Michael DH, O'Neill ME. 1970. Electrohydrodynamic instability in plane layers of fluid. *J. Fluid Mech.* 41:571–80
123. Min B, Ahn D. 2005. Mechanism of lipid peroxidation in meat and meat products—a review. *Food Sci. Biotechnol.* 14:152–63
124. Mir LM, Bureau MF, Gehl J, Rangara R, Rouy D, et al. 1999. High-efficiency gene transfer into skeletal muscle mediated by electric pulses. *PNAS* 96:4262–67
125. Moldovan L, Moldovan NI. 2004. Oxygen free radicals and redox biology of organelles. *Histochem. Cell Biol.* 122:395–412
126. Morrison PR, Ryser FA. 1952. Weight and body temperature in mammals. *Science* 116:231–32
127. Mussauer H, Sukhorukov AL, Haase A, Zimmermann U. 1999. Resistivity of red blood cells against high-intensity, short-duration electric field pulses induced by chelating agents. *J. Membrane Biol.* 170:121–33
128. Neamtu S, Morariu VV, Turcu I, Popescu AH, Copaescu LI. 1999. Pore resealing inactivation in electroporated erythrocyte membrane irradiated with electrons. *Bioelectrochem. Bioenerg.* 48:441–45
129. Needham D, Hochmuth RM. 1989. Electro-mechanical permeabilization of lipid vesicles. Role of membrane tension and compressibility. *Biophys. J.* 55:1001–9
130. Nesin V, Bowman AM, Xiao S, Pakhomov AG. 2012. Cell permeabilization and inhibition of voltage-gated Ca^{2+} and Na^{+} channel currents by nanosecond pulsed electric field. *Bioelectromagnetics* 33:394–404
131. Nesin V, Pakhomov AG. 2012. Inhibition of voltage-gated Na^{+} current by nanosecond electric field (nsPEF) is not mediated by Na^{+} influx or Ca^{2+} signaling. *Bioelectromagnetics* 33:443–51
132. Neu JC, Krassowska W. 1999. Asymptotic model of electroporation. *Phys. Rev. E* 59:3471–82
133. Neumann E, Kakorin S, Tönsing K. 1999. Fundamentals of electroporative delivery of drugs and genes. *Bioelectrochem. Bioenerg.* 48:3–16
134. Neumann E, Toensing K, Kakorin S, Budde P, Frey J. 1998. Mechanism of electroporative dye uptake by mouse B cells. *Biophys. J.* 74:98–108
135. Nörtemann K, Hilland J, Kaatze U. 1997. Dielectric properties of aqueous NaCl solutions at microwave frequencies. *J. Phys. Chem. A* 101:6864–69

136. Paganin-Gioanni A, Bellard E, Escoffre JM, Rols MP, Teissié J, Golzio M. 2011. Direct visualization at the single-cell level of siRNA electrotransfer into cancer cells. *PNAS* 108:10443–47
137. Pakhomov AG, Gianulis E, Vernier PT, Semenov I, Xiao S, Pakhomova ON. 2015. Multiple nanosecond electric pulses increase the number but not the size of long-lived nanopores in the cell membrane. *Biochim. Biophys. Acta* 1848:958–66
138. Pakhomov AG, Semenov I, Casciola M, Xiao S. 2017. Neuronal excitation and permeabilization by 200-ns pulsed electric field: an optical membrane potential study with FluoVolt dye. *Biochim. Biophys. Acta* 1859:1273–81
139. Pakhomov AG, Xiao S, Pakhomova ON, Semenov I, Kuipers AM, Ibey BL. 2014. Disassembly of actin structures by nanosecond pulsed electric field is a downstream effect of cell swelling. *Bioelectrochemistry* 100:88–95
140. Pakhomova ON, Khorokhorina VA, Bowman AM, Rodaitė-Riševičienė R, Saulis G, et al. 2012. Oxidative effects of nanosecond pulsed electric field exposure in cells and cell-free media. *Arch. Biochem. Biophys.* 527:55–64
141. Pavlin M, Leben V, Miklavčič D. 2007. Electroporation in dense cell suspension—theoretical and experimental analysis of ion diffusion and cell permeabilization. *Biochim. Biophys. Acta* 1770:12–23
142. Pedersen SF, Hoffmann EK, Mills JW. 2001. The cytoskeleton and cell volume regulation. *Comp. Biochem. Physiol. A* 130:385–99
143. Perrier DL, Rems L, Boukany PE. 2017. Lipid vesicles in pulsed electric fields: fundamental principles of the membrane response and its biomedical applications. *Adv. Colloid Interface Sci.* 249:248–71
144. Piggot TJ, Holdbrook DA, Khalid S. 2011. Electroporation of the *E. coli* and *S. aureus* membranes: molecular dynamics simulations of complex bacterial membranes. *J. Phys. Chem. B* 115:13381–88
145. Polak A, Bonhenry D, Dehez F, Kramar P, Miklavčič D, Tarek M. 2013. On the electroporation thresholds of lipid bilayers: molecular dynamics simulation investigations. *J. Membr. Biol.* 246:843–50
146. Polak A, Tarek M, Tomšič M, Valant J, Poklar Ulrih N, et al. 2014. Electroporation of archaeal lipid membranes using MD simulations. *Bioelectrochemistry* 100:18–26
147. Polak A, Velikonja A, Kramar P, Tarek M, Miklavčič D. 2015. Electroporation threshold of POPC lipid bilayers with incorporated polyoxyethylene glycol ($C_{12}E_8$). *J. Phys. Chem. B* 119:192–200
148. Portet T, Febrer FC, Escoffre JM, Favard C, Rols MP, Dean DS. 2009. Visualization of membrane loss during the shrinkage of giant vesicles under electropulsation. *Biophys. J.* 96:4109–21
149. Portet T, Mauroy C, Démery V, Houles T, Escoffre JM, Dean DS, Rols MP. 2012. Destabilizing giant vesicles with electric fields: an overview of current applications. *J. Membrane Biol.* 245:555–64
150. Prausnitz MR, Corbett JD, Gimm JA, Golan DE, Langer R, Weaver JC. 1995. Millisecond measurement of transport during and after an electroporation pulse. *Biophys. J.* 68:1864–70
151. Puc M, Kotnik T, Mir LM, Miklavčič D. 2003. Quantitative model of small molecules uptake after in vitro cell electropermeabilization. *Bioelectrochemistry* 60:1–10
152. Pucihar G, Kotnik T, Miklavčič D, Teissié J. 2008. Kinetics of transmembrane transport of small molecules into electropermeabilized cells. *Biophys. J.* 95:2837–48
153. Pucihar G, Kotnik T, Valič B, Miklavčič D. 2006. Numerical determination of transmembrane voltage induced on irregularly shaped cells. *Ann. Biomed. Eng.* 34:642–52
154. Raso J, Frey W, Ferrari G, Pataro G, Knorr D, et al. 2016. Recommendations guidelines on the key information to be reported in studies of application of PEF technology in food and biotechnological processes. *Innov. Food Sci. Emerg. Technol.* 37:312–21
155. Reale R, English NJ, Garate JA, Marracino P, Liberti M, Apollonio F. 2013. Human aquaporin 4 gating dynamics under and after nanosecond-scale static and alternating electric-field impulses: a molecular dynamics study of field effects and relaxation. *J. Chem. Phys.* 139:205101
156. Reigada R. 2014. Electroporation of heterogeneous lipid membranes. *Biochim. Biophys. Acta* 1838:814–21
157. Rems L, Miklavčič D. 2016. Tutorial: electroporation of cells in complex materials and tissue. *J. Appl. Phys.* 119:201101
158. Rems L, Tarek M, Casciola M, Miklavčič D. 2016. Properties of lipid electropores II: comparison of continuum-level modeling of pore conductance to molecular dynamics simulations. *Bioelectrochemistry* 112:112–24

159. Rems L, Viano M, Kasimova MA, Miklavčič D, Tarek M. 2019. The contribution of lipid peroxidation to membrane permeability in electropermeabilization: a molecular dynamics study. *Bioelectrochemistry* 125:46–57
160. Ren W, Sain NM, Beebe SJ. 2012. Nanosecond pulsed electric fields (nsPEFs) activate intrinsic caspase-dependent and caspase-independent cell death in Jurkat cells. *Biochem. Biophys. Res. Commun.* 421:808–12
161. Riske KA, Dimova R. 2005. Electro-deformation and poration of giant vesicles viewed with high temporal resolution. *Biophys. J.* 88:1143–55
162. Rols MP, Femenia P, Teissié J. 1995. Long-lived macropinocytosis takes place in electropermeabilized mammalian cells. *Biochem. Biophys. Res. Commun.* 208:26–35
163. Rols MP, Teissié J. 1990. Electropermeabilization of mammalian cells: quantitative analysis of the phenomenon. *Biophys. J.* 58:1089–98
164. Rols MP, Teissié J. 1992. Experimental evidence for the involvement of the cytoskeleton in mammalian cell electropermeabilization. *Biochim. Biophys. Acta* 1111:45–50
165. Rols MP, Teissié J. 1998. Electropermeabilization of mammalian cells to macromolecules: control by pulse duration. *Biophys. J.* 75:1415–23
166. Rosazza C, Deschout H, Buntz A, Braeckmans K, Rols MP, Zumbusch A. 2016. Endocytosis and endosomal trafficking of DNA after gene electrotransfer in vitro. *Mol. Ther. Nucl. Acids* 5:e286
167. Rosazza C, Haberl Meglić S, Zumbusch A, Rols MP, Miklavčič D. 2016. Gene electrotransfer: a mechanistic perspective. *Curr. Gene Ther.* 16:98–129
168. Roux B. 2008. The membrane potential and its representation by a constant electric field in computer simulations. *Biophys. J.* 95:4205–16
169. Saitta AM, Saija F, Giaquinta PV. 2012. Ab initio molecular dynamics study of dissociation of water under an electric field. *Phys. Rev. Lett.* 108:207801
170. Salomone F, Breton M, Leray I, Cardarelli F, Boccardi C, et al. 2014. High-yield nontoxic gene transfer through conjugation of the CM 18-Tat11 chimeric peptide with nanosecond electric pulses. *Mol. Pharm.* 11:2466–74
171. Scheffer HJ, Nielsen K, de Jong MC, van Tilborg AAJM, Viveen JM, et al. 2014. Irreversible electroporation for nonthermal tumor ablation in the clinical setting: a systematic review of safety and efficacy. *J. Vasc. Intervent. Radiol.* 25:997–1011
172. Schoenbach KH, Beebe SJ, Buescher ES. 2001. Intracellular effect of ultrashort electrical pulses. *Bioelectromagnetics* 22:440–48
173. Schutt EG, Klein DH, Mattrey RM, Riess JG. 2003. Injectable microbubbles as contrast agents for diagnostic ultrasound imaging: the key role of perfluorochemicals. *Angew. Chem. Int. Ed.* 42:3218–35
174. Sengel JT, Wallace MI. 2016. Imaging the dynamics of individual electropores. *PNAS* 113:5281–86
175. Shirakashi R, Sukhorukov VL, Tanasawa I, Zimmermann U. 2004. Measurement of the permeability and resealing time constant of the electroporated mammalian cell membranes. *Int. J. Heat Mass Transf.* 47:4517–4524
176. Smith KC, Neu JC, Krassowska W. 2004. Model of creation and evolution of stable electropores for DNA delivery. *Biophys. J.* 86:2813–26
177. Soh N, Makihara K, Ariyoshi T, Seto D, Maki T, et al. 2008. Phospholipid-linked coumarin: a fluorescent probe for sensing hydroxyl radicals in lipid membranes. *Anal. Sci.* 24:293–96
178. Son RS, Smith KC, Gowrishankar TR, Vernier PT, Weaver JC. 2014. Basic features of a cell electroporation model: illustrative behavior for two very different pulses. *J. Membrane Biol.* 247:1209–28
179. Sözer EB, Levine ZA, Vernier PT. 2017. Quantitative limits on small molecule transport via the electropermeome measuring and modeling single nanosecond perturbations. *Sci. Rep.* 7:57
180. Sözer EB, Pocetti CF, Vernier PT. 2018. Asymmetric patterns of small molecule transport after nanosecond and microsecond electropermeabilization. *J. Membr. Biol.* 251:197–210
181. Sözer EB, Pocetti CF, Vernier PT. 2018. Transport of charged small molecules after electropermeabilization—drift and diffusion. *BMC Biophys.* 11:4
182. Spugnini EP, Arancia G, Porrello A, Colone M, Formisano G, et al. 2007. Ultrastructural modifications of cell membranes induced by electroporation on melanoma xenografts. *Microsc. Res. Tech.* 70:1041–50

183. Stacey M, Fox P, Buescher S, Kolb J. 2011. Nanosecond pulsed electric field induced cytoskeleton, nuclear membrane and telomere damage adversely impact cell survival. *Bioelectrochemistry* 82:131–34
184. Sugár IP. 1979. A theory of the electric field-induced phase transition of phospholipid bilayers. *Biochim. Biophys. Acta* 556:72–85
185. Sugrue A, Maor E, Ivorra A, Vaidya V, Witt C, et al. 2018. Irreversible electroporation for the treatment of cardiac arrhythmias. *Expert Rev. Cardiovasc. Ther.* 16:349–360
186. Sunderman FW. 1945. Measurement of serum total base. *Am. J. Clin. Pathol.* 15:219–22
187. Szabo M, Wallace MI. 2016. Imaging potassium-flux through individual electropores in droplet interface bilayers. *Biochim. Biophys. Acta* 1858:613–617
188. Tarek M. 2005. Membrane electroporation: a molecular dynamics simulation. *Biophys. J.* 88:4045–53
189. Teissié J, Golzio M, Rols MP. 2005. Mechanisms of cell membrane electropermeabilization: a minireview of our present (lack of?) knowledge. *Biochim. Biophys. Acta* 1724:270–80
190. Teissié J, Rols MP. 1993. An experimental evaluation of the critical potential difference inducing cell membrane electropermeabilization. *Biophys. J.* 65:409–13
191. Teissié J, Tsong TY. 1980. Evidence of voltage-induced channel opening in Na/K ATPase of human erythrocyte membrane. *J. Membrane Biol.* 55:133–40
192. Teissié J, Tsong TY. 1981. Electric field induced transient pores in phospholipid bilayer vesicles. *Biochemistry* 20:1548–54
193. Tekle E, Astumian RD, Chock PB. 1994. Selective and asymmetric molecular transport across electroporated cell membranes. *PNAS* 91:11512–16
194. Tekle E, Oubrahim H, Dzekunov SM, Kolb JF, Schoenbach KH, Chock PB. 2005. Selective field effects on intracellular vacuoles and vesicle membranes with nanosecond electric pulses. *Biophys. J.* 89:274–84
195. Tieleman DP, Leontiadou H, Mark AE, Marrink SJ. 2003. Simulation of pore formation in lipid bilayers by mechanical stress and electric fields. *J. Am. Chem. Soc.* 125:6382–83
196. Tieleman DP. 2004. The molecular basis of electroporation. *BMC Biochem*. 5:10
197. Titushkin I, Cho M. 2009. Regulation of cell cytoskeleton and membrane mechanics by electric field: role of linker proteins. *Biophys. J.* 96:717–28
198. Tokman M, Lee JH, Levine ZA, Ho MC, Colvin ME, Vernier PT. 2013. Electric field-driven water dipoles: nanoscale architecture of electroporation. *PLOS ONE* 8(4):e61111
199. Towhidi L, Kotnik T, Pucihar G, Firoozabadi SMP, Mozdarani H, Miklavčič D. 2008. Variability of the minimal transmembrane voltage resulting in detectable membrane electroporation. *Electromagn. Biol. Med.* 27:372–85
200. Tsong TY. 1990. On electroporation of cell membranes and some related phenomena. *Bioelectrochem. Bioenerg.* 24:271–95
201. Tsong TY. 1991. Electroporation of cell membranes. *Biophys. J.* 60:297–306
202. Valko M, Rhodes CJ, Moncol J, Izakovic M, Mazur M. 2006. Free radicals, metals and antioxidants in oxidative stress-induced cancer. *Chem. Biol. Interact.* 160:1–40
203. Van der Paal J, Neyts EC, Verlackt CCW, Bogaerts A. 2016. Effect of lipid peroxidation on membrane permeability of cancer and normal cells subjected to oxidative stress. *Chem. Sci.* 7:489–98
204. van Uitert I, Le Gac S, van den Berg A. 2010. The influence of different membrane components on the electrical stability of bilayer lipid membranes. *Biochim. Biophys. Acta* 1798:21–31
205. Vasilkoski Z, Esser AT, Gowrishankar TR, Weaver JC. 2006. Membrane electroporation: the absolute rate equation and nanosecond time scale pore creation. *Phys. Rev. E* 74:021904
206. Vernier PT, Levine ZA, Wu YH, Joubert V, Ziegler MJ, et al. 2009. Electroporating fields target oxidatively damaged areas in the cell membrane. *PLOS ONE* 4:e7966
207. Weaver JC, Chizmadzhev YA. 1996. Theory of electroporation: a review. *Bioelectrochem. Bioenerg.* 41:135–60
208. Weaver JC, Vernier PT. 2017. Pore lifetimes in cell electroporation: complex dark pores? arXiv 1708.07478 [physics.bio-ph]
209. Wegner LH, Frey W, Silve A. 2015. Electroporation of DC-3F cells is a dual process. *Biophys. J.* 108:1660–71

210. Wojtaszczyk A, Caluori G, Pešl M, Melajova K, Stárek Z. 2018. Irreversible electroporation ablation for atrial fibrillation. *J. Cardiovasc. Electrophysiol.* 29:643–51
211. Wolf H, Rols MP, Boldt E, Neumann E, Teissié J. 1994. Control by pulse parameters of electric field-mediated gene transfer in mammalian cells. *Biophys. J.* 66:524–31
212. Wong-Ekkabut J, Xu Z, Triampo W, Tang IM, Tieleman DP, Monticelli L. 2007. Effect of lipid peroxidation on the properties of lipid bilayers: a molecular dynamics study. *Biophys. J.* 93:4225–36
213. Xiao D, Tang L, Yeng C, Wang J, Luo X, et al. 2011. Effect of actin cytoskeleton disruption on electric pulse-induced apoptosis and electroporation in tumour cells. *Cell Biol. Int.* 35:99–104
214. Yang L, Craviso GL, Vernier PT, Chatterjee I, Leblanc N. 2017. Nanosecond electric pulses differentially affect inward and outward currents in patch clamped adrenal chromaffin cells. *PLOS ONE* 12:e181002
215. Yarmush ML, Golberg A, Serša G, Kotnik T, Miklavčič D. 2014. Electroporation-based technologies for medicine: principles, applications, and challenges. *Annu. Rev. Biomed. Eng.* 16:295–320
216. Yeo SK, Liong MT. 2013. Effect of electroporation on viability and bioconversion of isoflavones in mannitol-soymilk fermented by lactobacilli and bifidobacteria. *J. Sci. Food Agric.* 93:396–409
217. Yoon J, Leblanc N, Zaklit J, Vernier PT, Chatterjee I, Craviso GL. 2016. Enhanced monitoring of nanosecond electric pulse-evoked membrane conductance changes in whole-cell patch clamp experiments. *J. Membrane Biol.* 249:633–44
218. Yun O, Zeng XA, Brennan CS, Han Z. 2016. Effect of pulsed electric field on membrane lipids and oxidative injury of *Salmonella typhimurium*. *Int. J. Mol. Sci.* 17:E1374
219. Zhao W, Yang R, Liang Q, Zhang W, Hua X, Tang Y. 2012. Electrochemical reaction and oxidation of lecithin under pulsed electric fields (PEF) processing. *J. Agric. Food Chem.* 60:12204–9